IEEE Access
Multidisciplinary ⋮ Rapid Review ⋮ Open Access Journal

Received March 4, 2021, accepted March 31, 2021, date of publication April 23, 2021, date of current version May 7, 2021.

Digital Object Identifier 10.1109/ACCESS.2021.3075274

A Lyapunov-Function Based Controller for 3-Phase Shunt Active Power Filter and Performance Assessment Considering Different System Scenarios

MOHIT BAJAJ[1], (Member, IEEE), AYMEN FLAH[2], MAJED ALOWAIDI[3], (Member, IEEE), NAVEEN KUMAR SHARMA[4], (Senior Member, IEEE), SHAILENDRA MISHRA[5], (Senior Member, IEEE), AND SUNIL KUMAR SHARMA[3]

[1]National Institute of Technology, Delhi 110040, India
[2]PEESE, National School of Engineering of Gabès, University of Gabès, Gabès 6029, Tunisia
[3]Department of Information Technology, College of Computer and Information Sciences, Majmaah University, Al Majmaah 11952, Saudi Arabia
[4]Department of Electrical Engineering, I. K. Gujral Punjab Technical University, Kapurthala 144603, India
[5]Department of Computer Engineering, College of Computer and Information Sciences, Majmaah University, Al Majmaah 11952, Saudi Arabia

Corresponding author: Sunil Kumar Sharma (s.sharma@mu.edu.sa)

The work of Sunil Kumar Sharma was supported by the Deanship of Scientific Research at Majmaah University under Project R-2021-97.

ABSTRACT Shunt active power filter (SAPF) belongs to the class of custom power devices (CPDs) and offers compensation to harmonics originated owing to customer side nonlinear loads, reactive power and unbalance in the distribution power networks functioning in current control mode (CCM). The performance of a SAPF as a harmonic compensator entirely relies on the control technique i.e. the precise detection of the harmonic current components of load that are necessary to be compensated. In the present work, a 3-phase SAPF, inspired by a Lyapunov function based control approach, has been designed for compensation of harmonics resulted in the feeder current owing to the customer side nonlinearity. A control law is determined in the proposed strategy which makes the derivative of the Lyapunov function consistently a negative one for an entire set of stable states. The DC-link capacitor voltage is regulated at constant reference through the proportional-integral (PI) controller. In this method rating of the shunt active power filter is considerably reduced than the other two broadly employed conventional methods. Furthermore, the harmonic compensation efficacy of the proposed Lyapunov function based SAPF is compared with the one based on other two conventional approaches under four different system scenarios namely a simple nonlinear load with and without utility side voltage distortion, a modified IEEE 13 bus test distribution system loaded with a 3-phase chopper fed direct current (DC) motor drive at a single bus and last especially for increasing the harmonic-constrained penetration level of renewable energy. Results obtained through simulation performed in MATLAB/Simulink shows that total harmonic distortion (THD) of source current and dynamic, as well as steady-state performance with Lyapunov function based controller, is significantly improved than the other two conventional methods. Also, the robust compensation performance of the SAPF empowers it to deal with the high penetration of renewable energy.

INDEX TERMS SAPF, Lyapunov function, harmonic compensation, hysteresis controller, renewable energy.

I. INTRODUCTION

Without a doubt the contemporary distribution power systems (DPS) tolerate high harmonic voltage and current distortions because of the intensified deployment of power electronics-based load equipment with nonlinear characteristics and analogous practices are being monitored at each of the DPS buses, for that reason, the notion of the standard and linear DPS has gone a quixotic one. That is a major and rising issue that the harmonic current interference and reactive power surge, the harmonic and reactive power control has turned into a matter of prevalent apprehension. The maximum

The associate editor coordinating the review of this manuscript and approving it for publication was Haiquan Zhao.

of the harmonic pollution concerns arisen in the distribution power network is as a consequence of the nonlinear nature of loads. The high customer side nonlinearity across the DPS has resulted in a substantial distortion in all buses' voltage and feeders' current owing to the aggregation of distortions of each bus with that of its buses acting as background [1]. In the present scenario, there is an increase in loads that are nonlinear and reactive in nature such as fans, electric pumps, TV, diode rectifier etc. [2]. The aforementioned loads increase reactive power burden and harmonic distortion in the distribution system. Furthermore, with the existence of widespread distributed generations (DGs), the situation from harmonic distortions viewpoint goes extra aggravated on account of harmonic current components injected by DG systems. Harmonic distortion in either voltage or current or both is irrefutably destructive to the DPS and this fact can be justified by life diminishing of distribution cables via harmonic de-rating, the unwarranted occurrence of power loss, false functioning of consumer appliances and industrial drives and finally and most importantly communication interference [3], [4]. The standard indices, used for measuring total along with individual order harmonic distortions in both PCC's voltage and line's current, must firmly adhere to IEEE Std. 519 and 1547 with and lacking the presence of distributed energy resources (DERs) [5]–[7]. Furthermore, despite being convincing for abundant applications, the mandatory penetration level of renewable energy has not been achieved yet remarkably because of the worsened harmonic performance of modern DPS in addition to some power quality (PQ) concerns linked with the DG systems themselves. The level of renewable energy penetration at which some of the harmonic constraints of the system begin to be disrupted is recognized as the system's harmonic-constrained hosting capacity (HC-HC) [8], [9]. The miserable harmonic performance of a DPS also highlights its meagre capacity for allowing the integration of renewable-based power.

To compensate reactive power burden and harmonic distortion various custom devices are used such as Shunt active power filter [10], [11], Static Compensator (STATCOM) [12], [13], Distribution Static Shunt Compensator (DSTATCOM) [14], Dynamic Voltage Restorer (DVR) [15], [16], Passive filter [17], Shunt Hybrid Active filter (SHAF) etc. Out of the plentiful of ways and power conditioning, CPDs for improving the quality of power and compensate harmonics, passive power filters (PPFs) are most widely adopted in DPS so as to compensate harmonic components of load currents. Besides the harmonic currents compensation, PPFs gives the provision of reactive power compensation, which can increase the power factor at PCC and thus resulting in abridged energy loss from reactive power flow and improved steady-state voltage profile at the PCC [18]. However, PPF based solution suffers from several drawbacks such as resonance, susceptibleness to utility and customer side distortion level, the dependence of feeder's stiffness and many more. Still, the PPF can be a better option when the economy is vital [19].

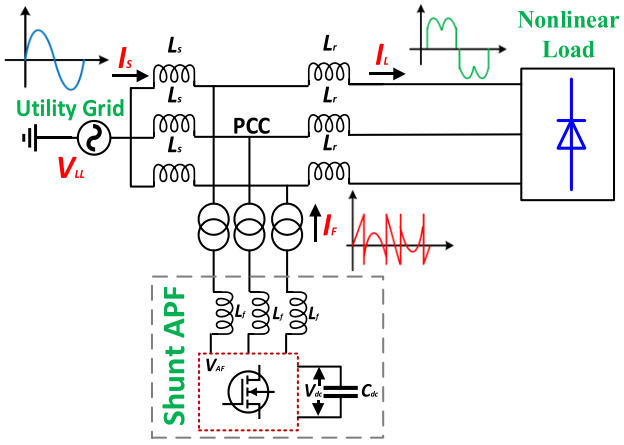

FIGURE 1. Basic diagram of SAPF.

At the same time, active filtering offers relief from all the issues associated with passive filtering but at the cost of complicated operation and budget. SAPF takes care of both the reactive power as well as harmonic constituents present in load current. SAPF is connected in shunt to mitigate harmonics and the reactive component of current and DVR is used to mitigate voltage related problem in the distribution system [20]. The amalgamation of both SAPF and DVR makes a Unified Power Quality Conditioner (UPQC) and the same mitigates both voltage in addition to a current related problem.

Figure 1 depicts the elementary compensation concept of a SAPF. A SAPF is controlled to either extract or injects a compensating current component I_F from/to the point of common coupling (PCC), with the aim of cancelling harmonics and reactive current components from the grid side and thereby sets the source side current a pure sinusoidal one and in line with the phase of source-side voltage.

There are different types of topologies for SAPF such as Voltage Source Converter (VSC) using 4-legs, 3-single phase VSC and VSC with 3-legs and a split type of capacitors. The SAPF has the following characteristics [21].

(a). It compensates harmonic currents.
(b). Operating in a harmonically polluted environment.
(c). Reactive current power compensation.
(d). Load balancing.
(e). Capacitor supported operation of SAPF.

When SAPF is employed for load's all-inclusive compensation, the accuracy of sensing the compensating current mandatory for the system is extremely significant for effective compensation, which depends on the control algorithm. There is various control algorithm has been used for SAPF in past such as Instantaneous Reactive Power (IRP) theory [22], Symmetrical Component (SC) theory, p-q theory, Synchronous Rotating Frame (SRF) theory [22], modified p-q theory [23], Average Unity Power Factor (AUPF) theory, adaptive control, Instantaneous Global Control Theory (IGCT), Average Global Control Theory (AGCT) [24] etc. The objectives of these theories are to extract fundamental components from load current and give the switching pulse

to VSC of SAPF such that it can track the harmonic and reactive component of load currents and thereby setting the source side current a pure sinusoidal one and in line with the phase of source-side voltage. There are many reference current detection techniques reported in the literature.

Akagi *et al.* [25] initially proposed Instantaneous reactive power theory in 1983, centred on a description of instantaneous real and reactive powers in the time domain and very useful for both three-phase systems with or without a neutral conductor, not only in the steady-state but also for transient analysis. Because of its precision, robustness and simple measurement, more than 60 per cent of research work considers using p-q theory at present. But the theory of p-q uses voltage signals to measure instantaneous active and reactive forces, any distortion and voltage imbalance will result in an incorrect measurement of reference source currents that should contain only the actual basic load current frequency portion and LPF used to filter the active power signal will cause compensation delay.

Bhattacharya *et al.* [26] then proposed synchronous reference frame theory in 1991, which was based on the transformation of the currents in synchronously rotating d-q frame. But the generation of voltage templates (sine and cosine) using PLL in synchronous reference frame theory plays an important role in the calculation of reference source currents. The tuning of the PLL is therefore important and the LPF used to filter the active power signal would trigger the compensation delay again.

In [27], the Symmetrical Components-based instantaneous power theory is suggested to avoid the limitation that the zero sequence components cannot be treated based on the method used in [25]. Once again, however, any distortion and voltage imbalance can lead to an incorrect measurement of reference source currents that should only contain the actual basic frequency portion of the load current.

Ghartemani *et al.* [28], A new phase-locked loop method, namely the enhanced phase-locked loop (EPLL) method in 2002, was then proposed. The suggested circuit can extract different information from an input signal, such as basic part, basic amplitude, basic phase angle, and frequency deviation, etc. The approach can be used to compensate for supply voltages that are both sinusoidal and distorted. But in order to get an appropriate transient response, the computation is very intensive and requires a careful setting of different parameters within the PLL. The compensator's transient response is very slow.

Mishra *et al.* [29], [30] then suggested a Fourier transformation based algorithm to produce the current of the reference source. Based on the well-known Fourier transform method, it is a very simple algorithm. Even under a skewed source voltage, this method may produce the reference source current. The technique can also provide a good half-cycle transient response because load current includes odd harmonics and even harmonics are included in one load current cycle.

Singh *et al.* [31] then proposed an Adaline based control algorithm, which was based on an artificial neural network in 2006. The basic theory of the proposed decomposer is based on the Least Mean Square (LMS) algorithm and thus requires less computational efforts to track the unit vector templates to maintain minimal error. Besides, the calculation delay caused by the processor is automatically compensated by this method. Once again, however, any distortion and voltage imbalance can lead to an incorrect measurement of reference source currents that should only contain the actual basic frequency portion of the load current.

Nair *et al.* [32] then proposed the Icosφ algorithm in 2006. The desired mains current is assumed in the Icosφ algorithm to be the product of the Icosφ magnitude and a sinusoidal wave unit amplitude in phase with the mains voltage. Only the active portion of the load current must be supplied by the mains, as the compensator is required to provide compensation for the harmonic and reactive portion of the three-phase load current and any difference in the balance. Therefore, from the mains, which will be strictly sinusoidal and in phase with the mains voltages, the only balanced current will be extracted. Once again, however, any distortion and voltage imbalance can lead to an incorrect measurement of reference source currents that should only contain the actual basic frequency portion of the load current.

So far, there are many approaches to determine the SAPF's reference compensation current. Most of them are based on reference frame transformation. The performance of SAPF units employing the conventional algorithms is not satisfactory and also dependent on the quality of voltage supplied from the utility side due to the assumption that the system's 3-phase voltage is copiously fundamental frequency and positive sequence component. Susceptibleness of performance of an active filter to such factors will also affect the perspective of high penetration of renewable energy in future DPS. The SAPF based on the new Lyapunov function tackles the challenge and gives promising results also in the case of imbalanced and non-sinusoidal supply-side voltage, compared to conventional SAPF based on traditional control techniques. In this paper reference filter, currents are generated with the help of p-q theory and SRF theory and a comparison is done of these approaches with new Lyapunov function inspired controller [33], [34] for SAPF. For tracking of current various kinds of controllers are used like sliding mode controller, hysteresis controller and pulse width modulation controller. Among these controllers, the hysteresis controller has been used in this paper for current tracking. The voltage of the DC-link capacitor is being regulated by using a Proportional-Integral (PI) controller. In this method, the voltage of the DC-link capacitor is subtracted from the reference voltage and fed to the input port of the PI controller. The Proportional-Integral controller maintains the DC-link capacitor voltage at the reference voltage [35].

The simulation model is also developed in MATLAB/Simulink environment. Results of simulations are compared with the other two compensation techniques based SAPF under four different scenarios. Under the first three scenarios, THD is compared among p-q theory [36], SRF method [37]

and Lyapunov function based control technique. In the fourth and last case, the enhanced penetration level of renewable energy by Lyapunov function based SAPF is compared with the one based on the other two compensation techniques. The switching pulses are produced by the hysteresis based controller to track the references current. Simulations are performed under various load condition such as a simple nonlinear load with and without utility side voltage distortion, a modified IEEE 13 bus test distribution system loaded with a 3-phase chopper fed direct current (DC) motor drive at a single bus and last especially for increasing the harmonic-constrained penetration level of renewable energy. The achieved results verify the usefulness of SAPF with the Lyapunov function inspired control technique in delivering harmonics compensation under different system scenarios.

The remaining segment of the article is prepared in the following fashion: Following the introductory part, the topology of the three-phase SAPF, on which the proposed controller has been implemented, is presented in section II. Section III describes the detailed modelling of the Lyapunov function based controller. Section IV throws a brief light on the mechanism of voltage control at the DC-link. Following the same, results under four considered scenarios are discussed in detail in section V. Section VI discusses the conclusion and future scope of work and references are listed in the end.

II. THE TOPOLOGY THREE PHASE SAPF

The topological schematic of a three-phase SAPF is depicted in Fig.2 [38]. It is a voltage source converter that consists of three legs. Each leg has two IGBT switches, connected with an anti-parallel diode. SAPF provides reactive as well as harmonic compensation. There is a DC-link capacitor across the VSC. The scale of the DC-link capacitor's capacitance should be very high. The voltage across the dc capacitor defined as,

$$\mathrm{Vdc} = \frac{2\sqrt{2}\mathrm{VLL}}{\sqrt{3}\mathrm{m}}$$

where V_{dc} is DC-link capacitor voltage, V_{LL} is source output line voltage and m is modulation index which is considered 1. Here V_{LL} is 415 volts. Thus V_{dc} is 677.69 in this paper. SAPF connected to the system with inductances because it removes the ripples from the compensator currents [39].

In figure 2, $[V_{sa}\ V_{sb}\ V_{sc}]^T$ and $[I_{sa}\ I_{sb}\ I_{sc}]^T$ are the vectors of source voltage and current respectively. $[I_{la}\ I_{lb}\ I_{lc}]^T$ is the vector of load current while $[I_{c1}\ I_{c2}\ I_{c3}]^T$ is the vector of compensator current. R and L are the resistance and inductance of interfacing VSC. $[V_{aP}\ V_{bP}\ V_{cP}]^T$ is the voltage vector at PCC.

It is controlled to either extract or inject a compensating current component i_c from/to the point of common coupling (PCC), with the aim of cancelling harmonics and reactive current components from the grid side, and thereby sets the source side current a pure sinusoidal one and in line with the phase of source-side voltage [39].

III. LYAPUNOV THEORY BASED CONTROL ALGORITHM

According to the Lyapunov method, SAPF energy reduces along the trajectories of the system. Lyapunov stability theorem conditions that a nonlinear system is universally asymptotically stable in case Lyapunov function $V(x)$ fulfils these properties:

$$\begin{cases} V\,(0) & \\ V\,(x) > 0 & \text{for all } x \neq 0 \\ \dot{V}\,(x) < 0 & \text{for all } x \neq 0 \\ V\,(x) \to \infty & \text{as } \|x\| \to \infty \end{cases}$$

The Lyapunov function for SAPF defined as stored energy in it and is a positive definite function. Now considering the SAPF model shown in figure 2.

$$\mathrm{V_{sa}} = \mathrm{L}\frac{\mathrm{di_{c1}}}{\mathrm{dt}} + \mathrm{Ri_{c1}} + \mathrm{V_{aP}} + \mathrm{V_{PQ}} \tag{1}$$

$$\mathrm{V_{sb}} = \mathrm{L}\frac{\mathrm{di_{c2}}}{\mathrm{dt}} + \mathrm{Ri_{c2}} + \mathrm{V_{bP}} + \mathrm{V_{PQ}} \tag{2}$$

$$\mathrm{V_{sc}} = \mathrm{L}\frac{\mathrm{di_{c3}}}{\mathrm{dt}} + \mathrm{Ri_{c3}} + \mathrm{V_{cP}} + \mathrm{V_{PQ}} \tag{3}$$

$$\frac{\mathrm{dV_{dc}}}{\mathrm{dt}} = \frac{1}{\mathrm{C_{dc}}}\mathrm{i_{dc}} \tag{4}$$

We assume that the source is balanced hence

$$\mathrm{V_{sa}} + \mathrm{V_{sb}} + \mathrm{V_{sc}} = 0 \tag{5}$$

$$\mathrm{V_{PQ}} = -\frac{1}{3}\sum_{\mathrm{n}=1}^{3}\mathrm{V_{nP}} \tag{6}$$

The switching function of i^{th} leg of the voltage source converter

$$\mathrm{c_i} = \begin{cases} 1 \\ 0 \end{cases} \tag{7}$$

$$\mathrm{V_{iP}} = \mathrm{c_i V_{dc}} \tag{8}$$

The i^{th} phase dynamic equation of SAPF model is given by

$$\frac{\mathrm{di_{ci}}}{\mathrm{dt}} = -\frac{\mathrm{R}}{\mathrm{L}}\mathrm{i_{ci}} - \frac{1}{\mathrm{L}}\left(\mathrm{c_i} - \frac{1}{3}\sum_{\mathrm{n}=1}^{3}\mathrm{c_n}\right)\mathrm{V_{dc}} + \frac{\mathrm{V_{si}}}{\mathrm{L}} \tag{9}$$

A switching state function is given by

$$\mathrm{d_{mi}} = \left(\mathrm{c_i} - \frac{1}{3}\sum_{\mathrm{n}=1}^{3}\mathrm{c_n}\right)_{\mathrm{m}} \tag{10}$$

Based on eq. (10), conversion from c_i to d_{mi} is given by

$$\begin{bmatrix} \mathrm{d_{m1}} \\ \mathrm{d_{m2}} \\ \mathrm{d_{m3}} \end{bmatrix} = \begin{bmatrix} 2 & -1 & -1 \\ -1 & 2 & -1 \\ -1 & -1 & 2 \end{bmatrix} \begin{bmatrix} \mathrm{c_1} \\ \mathrm{c_2} \\ \mathrm{c_3} \end{bmatrix} \tag{11}$$

Analysis of the DC component of the model

$$\frac{\mathrm{dV_{dc}}}{\mathrm{dt}} = \frac{1}{\mathrm{C_{dc}}}\mathrm{i_{dc}} = \frac{1}{\mathrm{C_{dc}}}\sum_{\mathrm{n}=1}^{3}\mathrm{c_n i_{cn}} \tag{12}$$

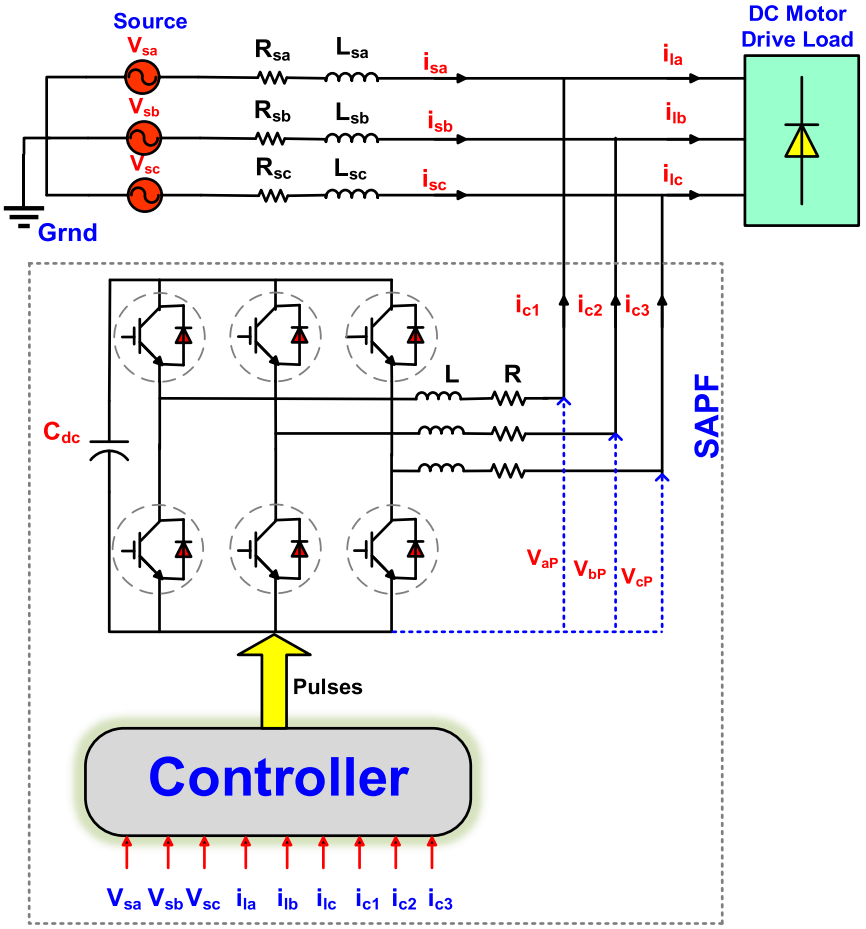

FIGURE 2. Configuration of SAPF.

TABLE 1. Value of α versus THD and S.S. response.

Value of α	-3	-1	-0.1
%THD	2.89	4.78	18.31
S.S. Response Time (in a sec)	0.07	0.07	0.5

It can be proved that

$$\sum_{n=1}^{3} d_{mn} i_{cn} = \sum_{n=1}^{3} c_n i_{cn} \tag{13}$$

From eq. (13) we can obtain the relation

$$\frac{dV_{dc}}{dt} = \frac{1}{C_{dc}} \sum_{n=1}^{3} d_{mn} i_{cn} \tag{14}$$

Due to the nonexistence of zero sequence current in ac currents and in $[d_{mi}]$ function lead to this differential equation on the dc side

$$\frac{dV_{dc}}{dt} = \frac{1}{C_{dc}} [2d_{n1} + d_{n2}] i_{c1} + \frac{1}{C_{dc}} [d_{n1} + 2d_{n2}] i_{c2} \tag{15}$$

TABLE 2. Parameters of the test system.

Parameters	Value
Supply Voltage	415 V (L-L), 50 Hz.
RL Balanced Load	$R = 26\ \Omega$, $L = 2$mH
Non-linear Load	3-phase full-wave rectifier drawing a dc current of 2.8 A
DC-Link Capacitor	2000 μF
Interface inductor	$L_f = 30$ mH , $R_f = 0.4\ \Omega$
Reference DC-link Voltage	$V^*_{dc} = 700$
PI-Controller Gains	$K_p = 15$, $K_i = 0.7$
feeder Parameters	$L_s = 0.5$ mH , $R_s = 0.8294\ \Omega$

The complete model of three-phase SAPF is obtained from

$$\frac{d}{dt}\begin{bmatrix} i_{c1} \\ i_{c2} \\ V_{dc} \end{bmatrix} = \begin{bmatrix} -\frac{R}{L} & 0 & -\frac{d_{m1}}{L} \\ 0 & -\frac{R}{L} & -\frac{d_{m2}}{L} \\ \frac{2d_{m1}+d_{m2}}{C_{dc}} & \frac{d_{m1}+2d_{m2}}{C_{dc}} & 0 \end{bmatrix} \times \begin{bmatrix} i_{c1} \\ i_{c2} \\ V_{dc} \end{bmatrix} + \frac{1}{L}\begin{bmatrix} V_{sa} \\ V_{sb} \\ 0 \end{bmatrix} \tag{16}$$

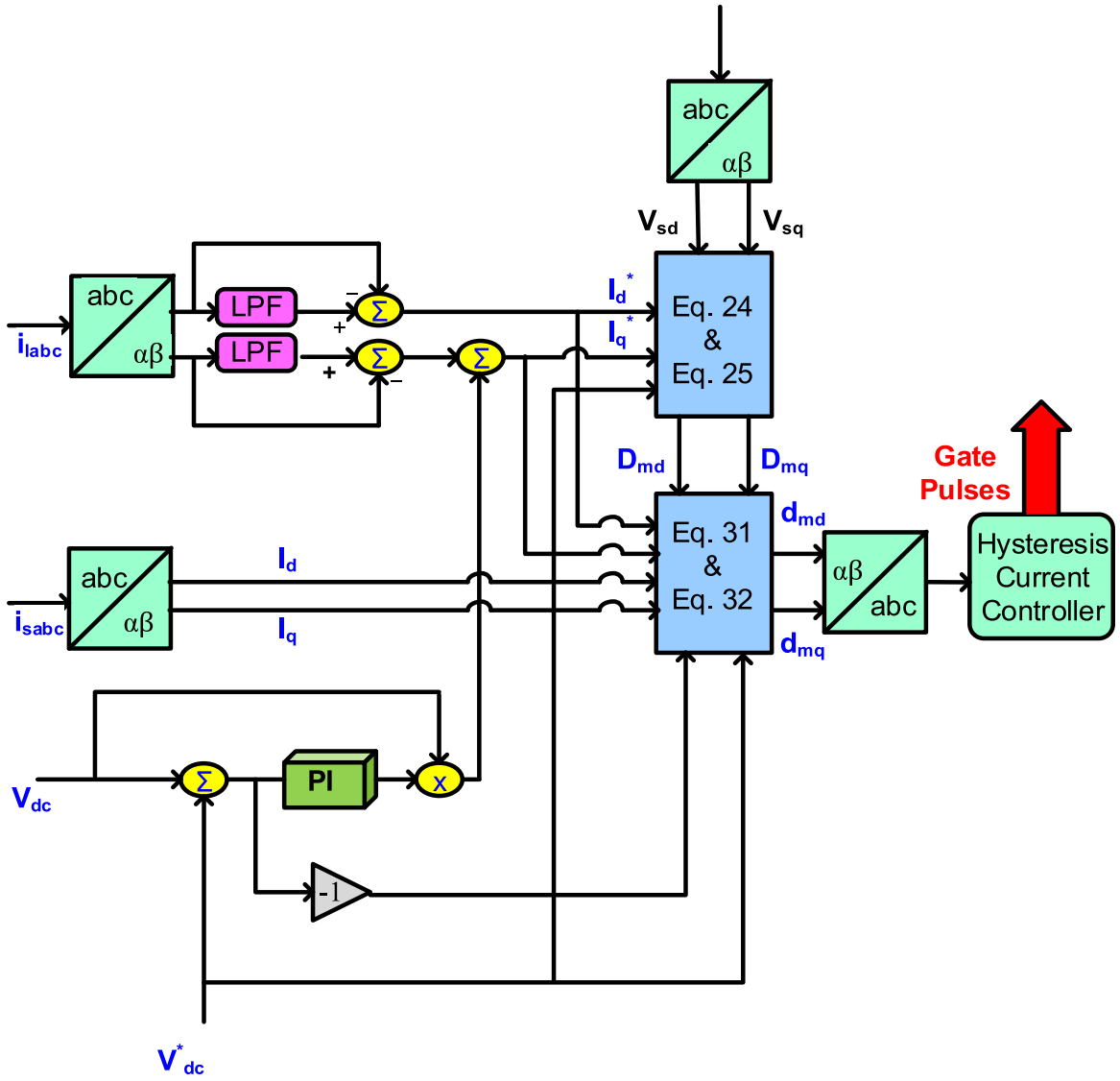

FIGURE 3. Control strategy of Lyapunov function based controller.

Using the SRF (Synchronous Rotating Frame) theory, three-phase quantities converted into two-phase quantities. The transformation matrix is given by

$$A_{dq}^{123} = \sqrt{\frac{2}{3}} \begin{bmatrix} \cos\theta & \cos\left(\theta - \frac{2\pi}{3}\right) & \cos\left(\theta - \frac{4\pi}{3}\right) \\ -\sin\theta & -\sin(\theta - \frac{2\pi}{3}) & -\sin(\theta - \frac{4\pi}{3}) \end{bmatrix} \tag{17}$$

where, $\theta = \omega t$.

The resulting transformed model is given by

$$\frac{di_d}{dt} = -\frac{R}{L} i_d + \omega i_q - \frac{d_{md}}{L} V_{dc} + \frac{1}{L} V_{sd} \tag{18}$$

$$\frac{di_q}{dt} = -\frac{R}{L} i_q - \omega i_d - \frac{d_{mq}}{L} V_{dc} + \frac{1}{L} V_{sq} \tag{19}$$

$$\frac{dV_{dc}}{dt} = \frac{d_{md}}{C_{dc}} i_d + \frac{d_{mq}}{C_{dc}} i_q \tag{20}$$

For setting the state-space model, let us choose the state variable as

$$x_1 = i_d - i_d^*, \quad x_2 = i_q - i_q^*, \; x_3 = V_{dc} - V_{dc}^*$$

The complete model equations in terms of x_1, x_2 and x_3 are given by

$$\frac{dx_1}{dt} = -\frac{R}{L} x_1 + \omega x_2 - \frac{1}{L} d_{md} \left(x_3 + V_{dc}^*\right) - \frac{D_{md}}{L} V_{dc}^* \tag{21}$$

$$\frac{dx_2}{dt} = -\frac{R}{L} x_2 - \omega x_1 - \frac{1}{L} d_{mq} \left(x_3 + V_{dc}^*\right) - \frac{D_{mq}}{L} V_{dc}^* \tag{22}$$

$$\frac{dx_3}{dt} = \frac{1}{C_{dc}} \left[d_{md} \left(x_1 + i_d^*\right) + d_{mq} \left(x_2 + i_q^*\right) + D_{md} i_d^* + D_{mq} i_q^* \right] \tag{23}$$

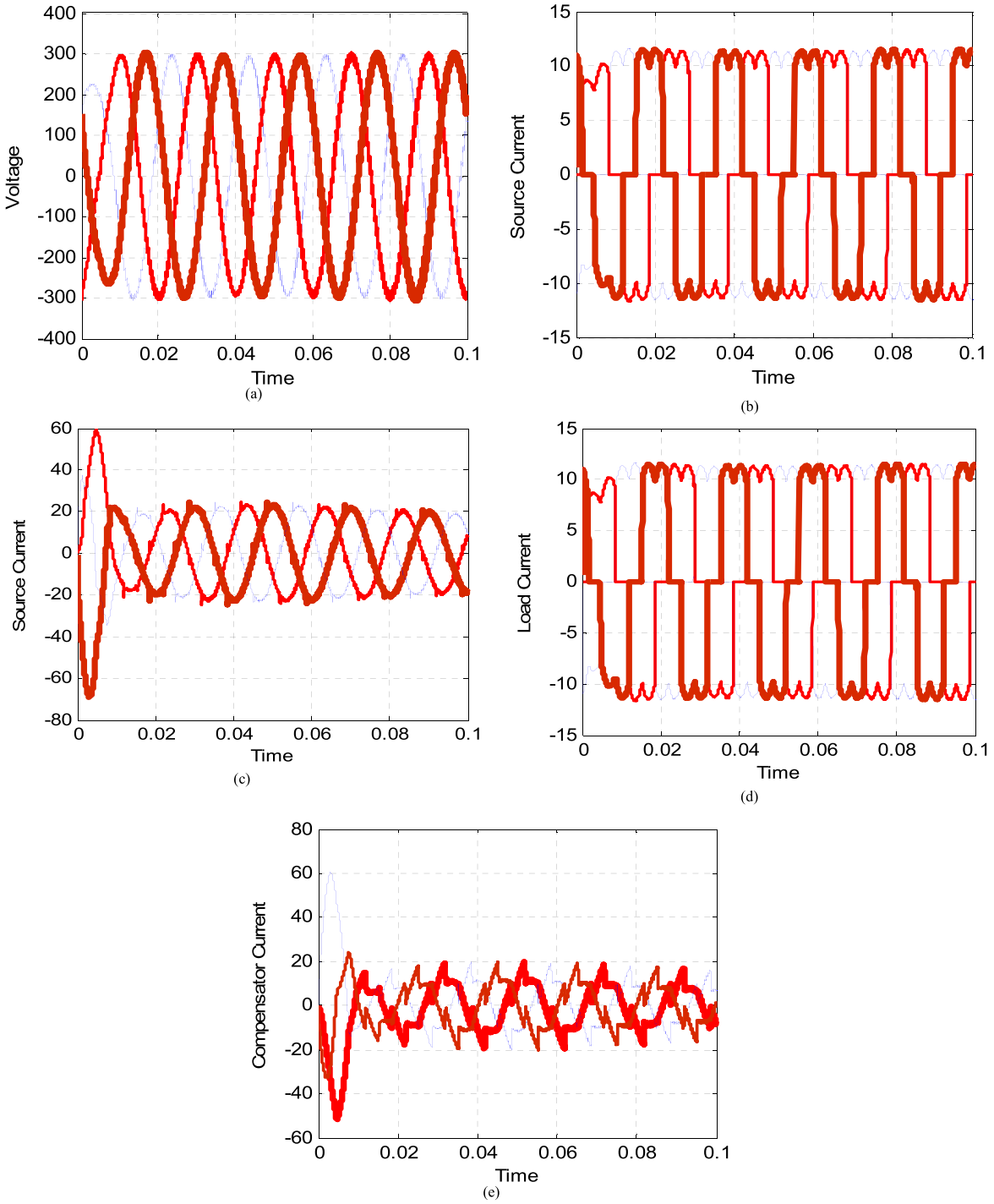

FIGURE 4. Waveforms of p-q theory (a-b) before and (c-e) after compensation.

where i_d^*, i_q^* are references taken out from nonlinear load's total current and V_{dc}^* are reference DC-link capacitor voltage. D_{md} and D_{mq} are steady-state switching function and given by the following equations

$$D_{md} = \frac{L}{V_{dc}^*}\left[-\frac{di_d^*}{dt} - \frac{R}{L}i_d^* + \omega i_q^* + \frac{1}{L}V_{sd}\right] \tag{24}$$

$$D_{mq} = \frac{L}{V_{dc}^*}\left[-\frac{di_q^*}{dt} - \frac{R}{L}i_q^* + \omega i_d^* + \frac{1}{L}V_{sq}\right] \tag{25}$$

Now, the role of the concept of Lyapunov function comes in and according to it

$$V = \frac{3}{2}Lx_1^2 + \frac{3}{2}Lx_2^2 + \frac{1}{2}C_{dc}x_3^2 \tag{26}$$

This system is globally stable if derivative of eq. (26) is negative.

$$\frac{dV}{dt} = 3x_1\left[-Rx_1 + L\omega x_2 - d_{md}\left(x_3 + V_{dc}^*\right) - D_{md}V_{dc}^*\right]$$

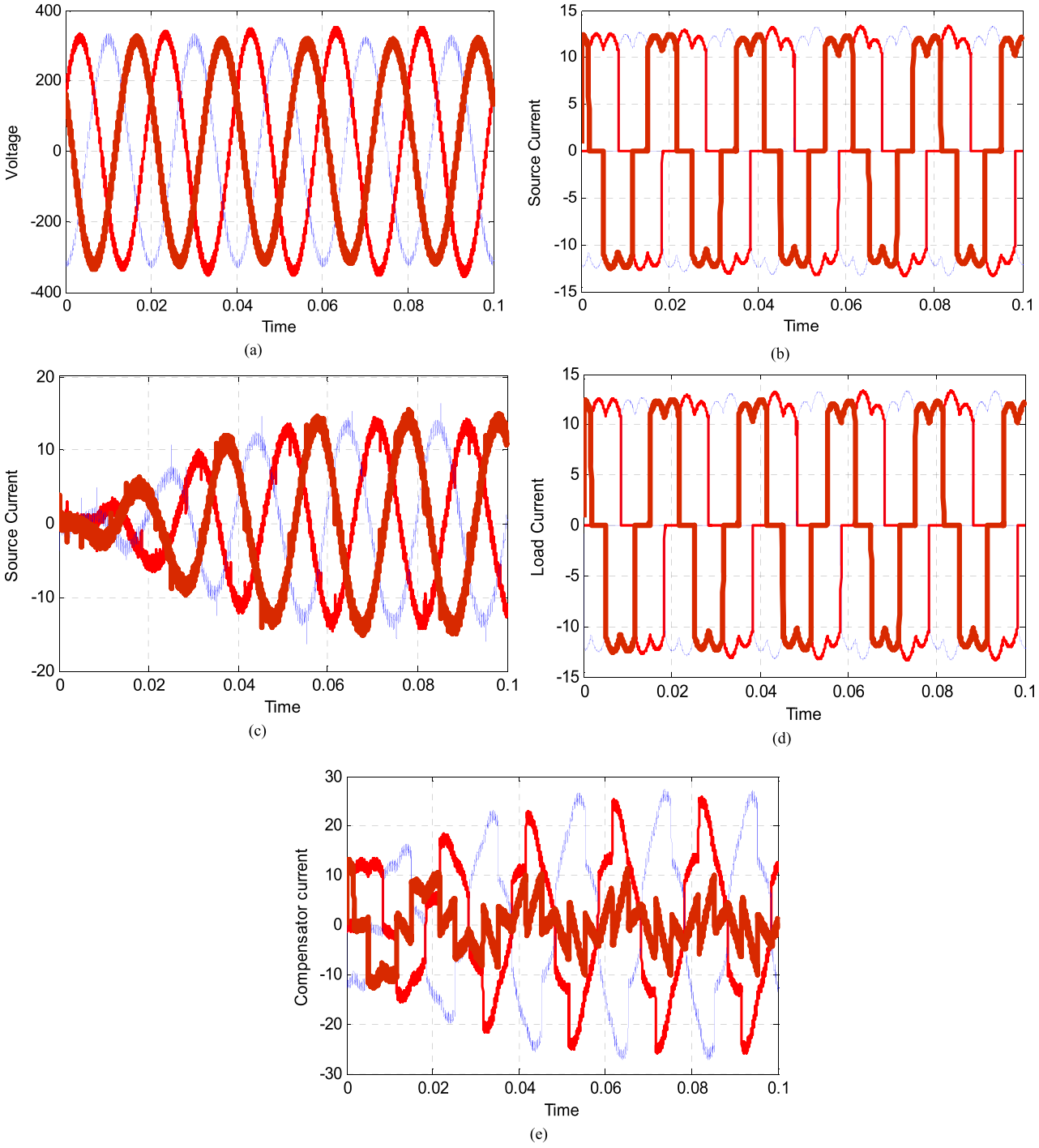

FIGURE 5. Waveforms of SRF theory (a-b) before and (c-e) after compensation.

$$+3x_2\left[-Rx_2-L\omega x_1-d_{mq}\left(x_3+V_{dc}^*\right)-D_{mq}V_{dc}^*\right]+x_3\left[d_{md}\left(x_1+i_d^*\right)\right]+d_{mq}\left(x_2+i_q^*\right)+D_{md}i_d^*+D_{mq}i_q^* \quad (27)$$

The above equation can be expressed in this subsequent form

$$\frac{dV}{dt}=-3Rx_1^2-3Rx_2^2+d_{md}\left(x_3i_d^*-3x_1V_{dc}^*\right)+d_{mq}\times\left(x_3i_q^*-3x_2V_{dc}^*\right)+D_{md}(x_3i_d^*-3x_1V_{dc}^*)+D_{mq}\times\left(x_3i_q^*-3x_2V_{dc}^*\right) \quad (28)$$

The above equation can be articulated as

$$\frac{dV}{dt}=-3Rx_1^2-3Rx_2^2+d_{md}\left[x_3i_d^*-3x_1\left(V_{dc}^*+\frac{2}{3}x_3\right)\right]+d_{mq}\left[x_3i_q^*-3x_2\left(V_{dc}^*+\frac{2}{3}x_3\right)\right]$$

We know that

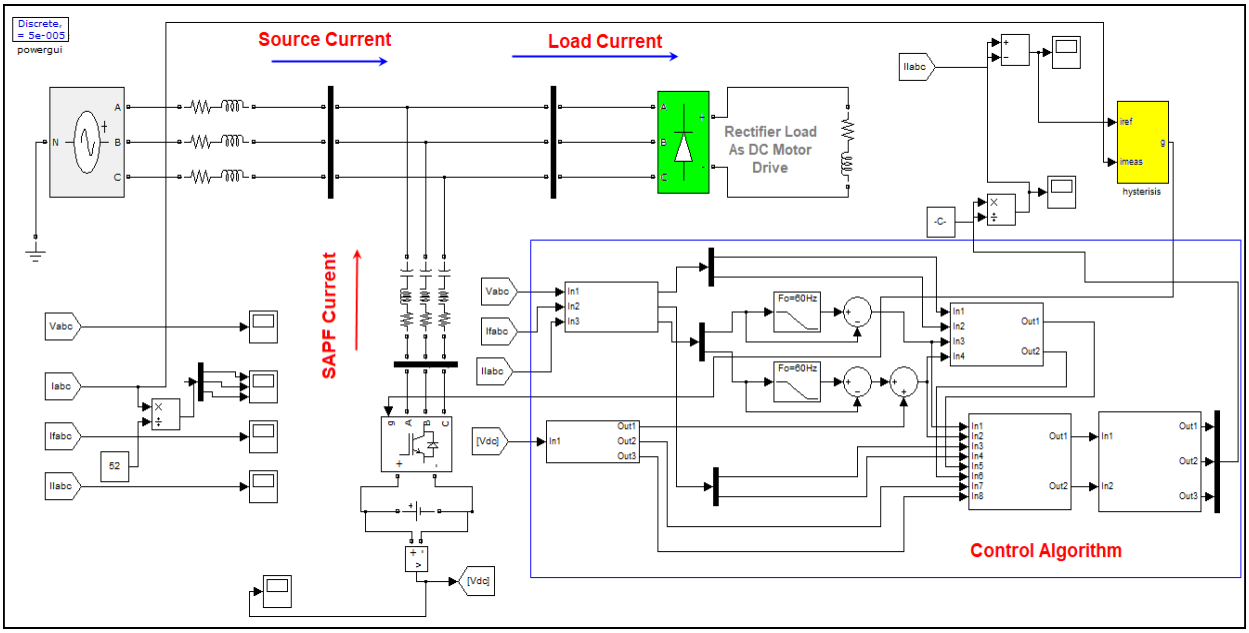

FIGURE 6. Matlab/Simulink based model of Lyapunov function based control technique.

$V_{dc}^* \gg x_3$ and

$$V_{dc}^* + \frac{2}{3}x_3 \cong V_{dc}^* \tag{29}$$

Then eq. (28) becomes

$$\frac{dV}{dt} = -3Rx_1^2 - 3Rx_2^2 + (d_{md} + D_{md})\left(x_3 i_d^* - 3x_1 V_{dc}^*\right) + (d_{mq} + D_{mq})\left(x_3 i_q^* - 3x_2 V_{dc}^*\right) \tag{30}$$

The first two terms in eq. (30), $-3Rx_1^2$, $-3Rx_2^2$ are negative

$$d_{md} = \alpha\left(x_3 i_d^* - 3x_1 V_{dc}^*\right) - D_{md} \tag{31}$$

$$d_{mq} = \alpha\left(x_3 i_q^* - 3x_2 V_{dc}^*\right) - D_{mq} \tag{32}$$

where α is the controller gain of SAPF. Figure 3 shows the entire mechanism of reference current generation by the Lyapunov function based controller in SAPF.

A. CHOICE OF CONTROLLER GAIN α

The value of α should be negative to be system stable. Choice of α affects the performance of the compensator as shown in Table-1. As the value of α increase, THD and steady-state response time is decreased. In the case of α being lessor than -1, the response time remains unpretentious though THD decrease.

IV. REGULATION OF DC-LINK CAPACITOR VOLTAGE

There occurs some real power loss on the dc side capacitor owing to the high-speed switching of power electronics switches in 3-phase VSC. The arrangement of the provision of such switching loss becomes mandatory because if not done so the hysteresis loop controller fails to track the generated reference current owing to fluctuations in DC-link voltage. To compensate for these losses, we require a regulation mechanism for dc side voltage [11]. Hence DC-link voltage is necessary to be maintained constant in order to ensure accurate tracking of reference current by the compensation current. To regulate these losses, we used a proportional-integral (PI), controller. Though the application of these controllers causes steady-state errors, and the inadequacy of bandwidth has not permitted reasonable harmonic compensation. The value of dc capacitors is designated on the basis of its capacity to adjust voltage throughout transients. The output of the PI controller is added to the q component extracted from the load current. The addition of yield of PI controller with the average magnitude of the active component of the load currents is the total active components of the reference source current. The controller parameters are chosen such that it stabilizes the V_{dc} around the V_{dc}^*. The output of PI controller can be computed as

$$i_d(n) = i_d(n-1) + K_d\left(V_{dc}^*(n) - V_{dc}(n-1)\right) + K_i V_{dce} \tag{33}$$

$$V_{dce} = V_{dc}^* - V_{dc} \tag{34}$$

V. SIMULATION RESULTS AND DISCUSSION

The performance of the Lyapunov Function-based Controller of SAPF has been tested under four systems scenarios. All the simulations are carried out using MATLAB/Simulink software. To assess the performance of the Lyapunov Function-based Controller of SAPF, the system is analyzed before and after compensation under all four system scenarios. The specification parameters of the system employed for analysis under case-1, in the MATLAB simulation, are shown in Table 2 [40]. In case-1 the proposed SAPF is first tested on a two-bus system with a 3-phase rectifier type load. Also, the utility side is also assumed fully fundamental

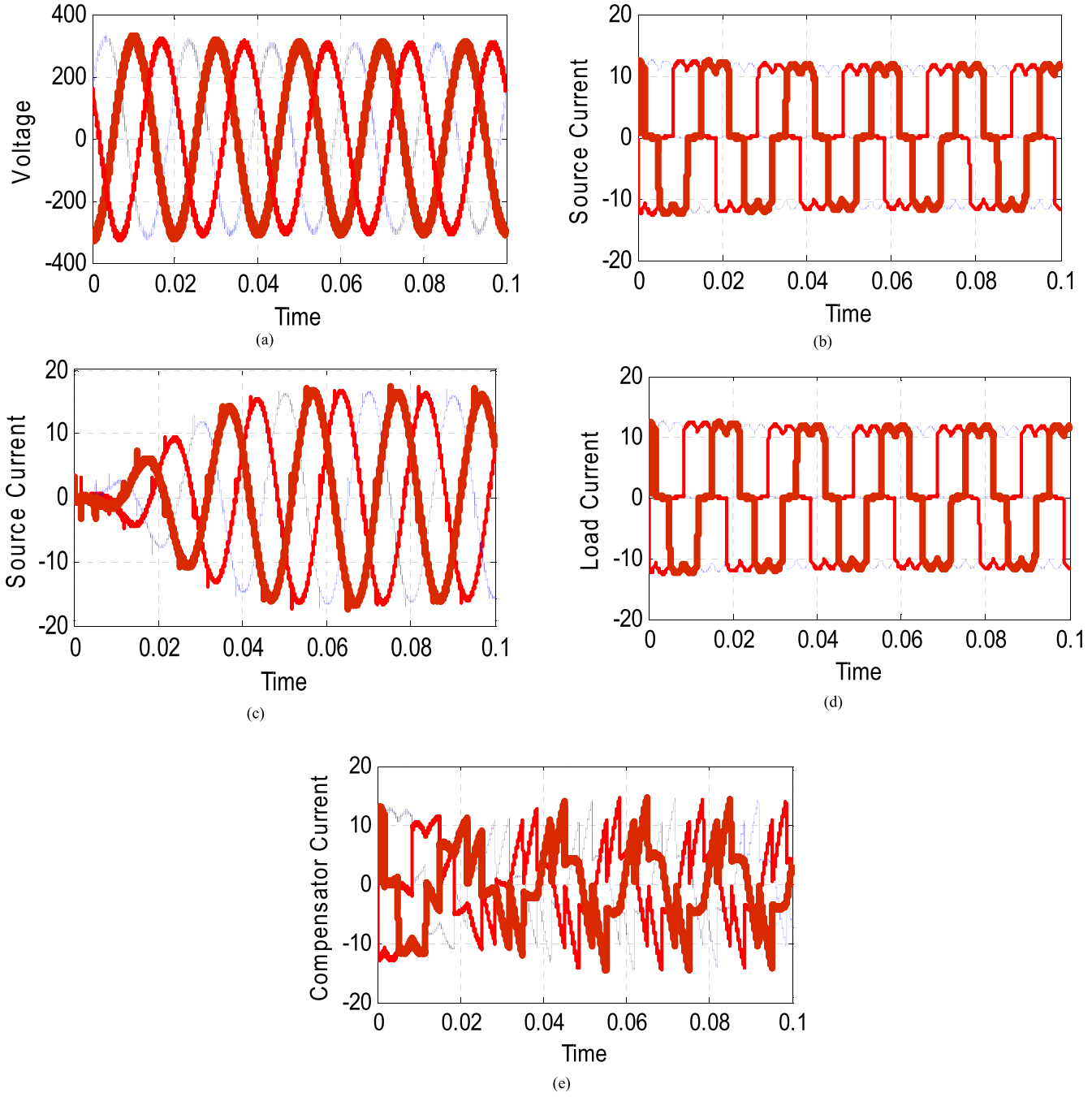

FIGURE 7. Waveforms of Lyapunov function based control technique (a-b) before and (c-e) after compensation.

positive sequence at 415 Volt RMS line to line and free from any nonlinearity or unbalance. Accordingly, reference DC link voltage is taken as 700 Volt. The value of the DC-link capacitor is taken as 2000 μF. The associated constants of PI controller gains are selected by hit and trial and kept fixed at 15 and 0.7 respectively. However, the technical specification of the system in each of the scenarios is considered quite different.

The waveforms of the p-q theory are shown in figure 4 (a-e) before as well as after compensation. Considering the stiffness of the feeder as per table 2, the voltage at PCC is identical to that of the source itself. Waveforms 4 (a-b) belongs to the before compensation case. For an uncompensated system since load current is identical to the source current hence load current waveform has not been displayed separately. The waveform of the source or load current clearly depicts the harmonics present in the same. With the connection of the p-q theory controlled SAPF, the quality of source current waveforms can be clearly distinguished from the load current. However,

owing to the limitation of the p-q theory-based controller source current is not closer to the pure sinusoidal one yet its THD in each phase lies under the limits specified by IEEE Std. 519.

The transients can be witnessed in the source current from the period of 0 sec to approximately 0.01 sec especially with p-q theory controlled SAPF also forms a significant base of comparison among the three simulated techniques. One probable cause of such transient in the source currents is the slow buildup of voltage across the DC-link capacitor.

The waveforms of the SRF theory are depicted in figure 5(a-e) before and after compensation. Because of the stiffness of the feeder according to table 2, the voltage at PCC is indistinguishable from that of the source itself. Such scenarios exacerbate the PQ condition in the distribution feeders leading to their de-rating under the presence of harmonics. Waveforms 5 (a-b) belongs to the before compensation case. Again for an uncompensated system since load current is identical to the source current therefore load current waveform has not been presented individually. Waveforms 5 (c-e) belongs to the after compensation case. Under the presence of SAPF, the source current waveforms can be clearly differentiated from the load current. Yet due to the imperfection of SRF based controller source current is not closer to the pure sinusoidal one though it's THD exists under the limits specified by IEEE Std. 519.

The transients can be again witnessed in the source current from the period of 0 sec to approximately 0.01 sec with SRF theory controlled SAPF also but relatively lesser than p-q theory-based controller.

Figure 6 depicts the MATLAB/Simulink based model of Lyapunov function inspired control technique for load compensation using SAPF. The waveforms of the Lyapunov function based control technique are shown in figure 7 (a-e) before and after compensation. Waveforms 7 (a-b) belongs to the before compensation case. Again for an uncompensated system since load current is identical to the source current therefore load current waveform has not been presented individually. Waveforms 7 (c-e) belongs to the after compensation case. With the connection of the Lyapunov function controlled SAPF, the quality of source current waveforms can be clearly distinguished from the load current. However, again owing to the limitation of reference current tracking of hysteresis loop controller source current is not closer to the pure sinusoidal one yet its THD in each phase lies under the limits specified by IEEE Std. 519 and better than p-q and SRF theory.

THD of phase-A of source current, before and after compensation, is depicted in figure 8. The THD of source current by the Lyapunov function based control technique is reduced from 30.04% to 1.61% in phase-a. While the same is reduced from 29.18% to 3.19% with the well-known p-q theory and from 28.89% to 4.88% with the SRF theory. It becomes evident that the source current with the Lyapunov function based SAPF installed at the PCC is rather closer to the desired purely sinusoidal one.

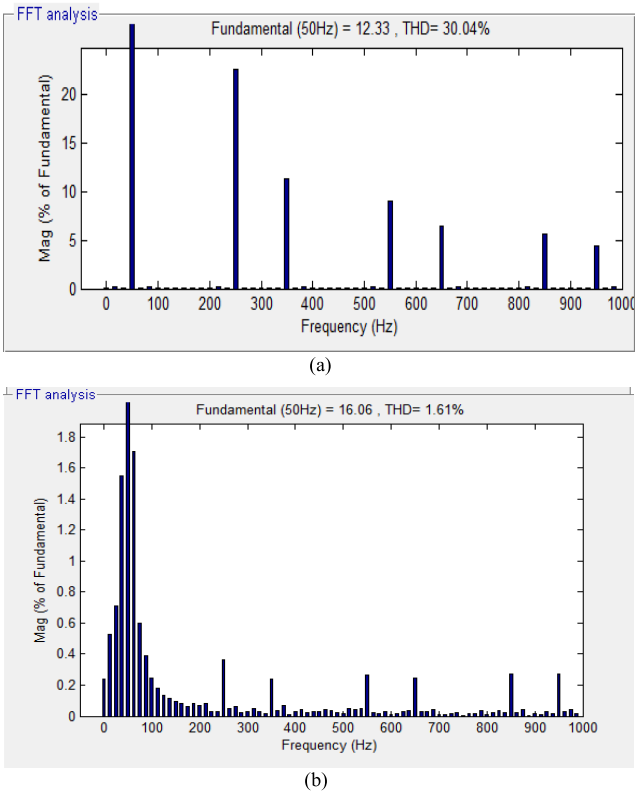

FIGURE 8. FFT analysis a) Before compensation, b) After compensation.

TABLE 3. Comparison of control algorithms.

S. No.	Control Algorithm	%THD					
		Before Compensation			After Compensation		
		Phase A	Phase B	Phase C	Phase A	Phase B	Phase C
1.	p-q theory	29.18	29.32	28.25	3.19	2.73	3.05
2.	SRF theory	28.89	27.63	31.60	4.88	4.80	4.65
3.	Lyapunov function	30.04	29.44	29.55	1.61	2.33	1.99

Comparing the waveforms of source current i.e. 4(c), 5(c) and 7(c), it can be inferred that the Lyapunov function based control technique offers a better steady-state response. Rise time offered by the Lyapunov function based control technique is also somewhat lessor that the two conventional ones.

Figure 4(c) shows the occurrence of high overshoot in the source current in the case of p-q theory. While the same is nearly absent in the response of the other two theories. The little transients can be again witnessed in the source current from the period of 0 sec to approximately 0.01 sec with Lyapunov function based control theory but relatively lesser than both p-q theory and SRF theory-based controller.

Under the second scenario of the system or Case-2, the performance of the proposed Lyapunov function controlled SAPF is tested under utility or source-side disturbances.

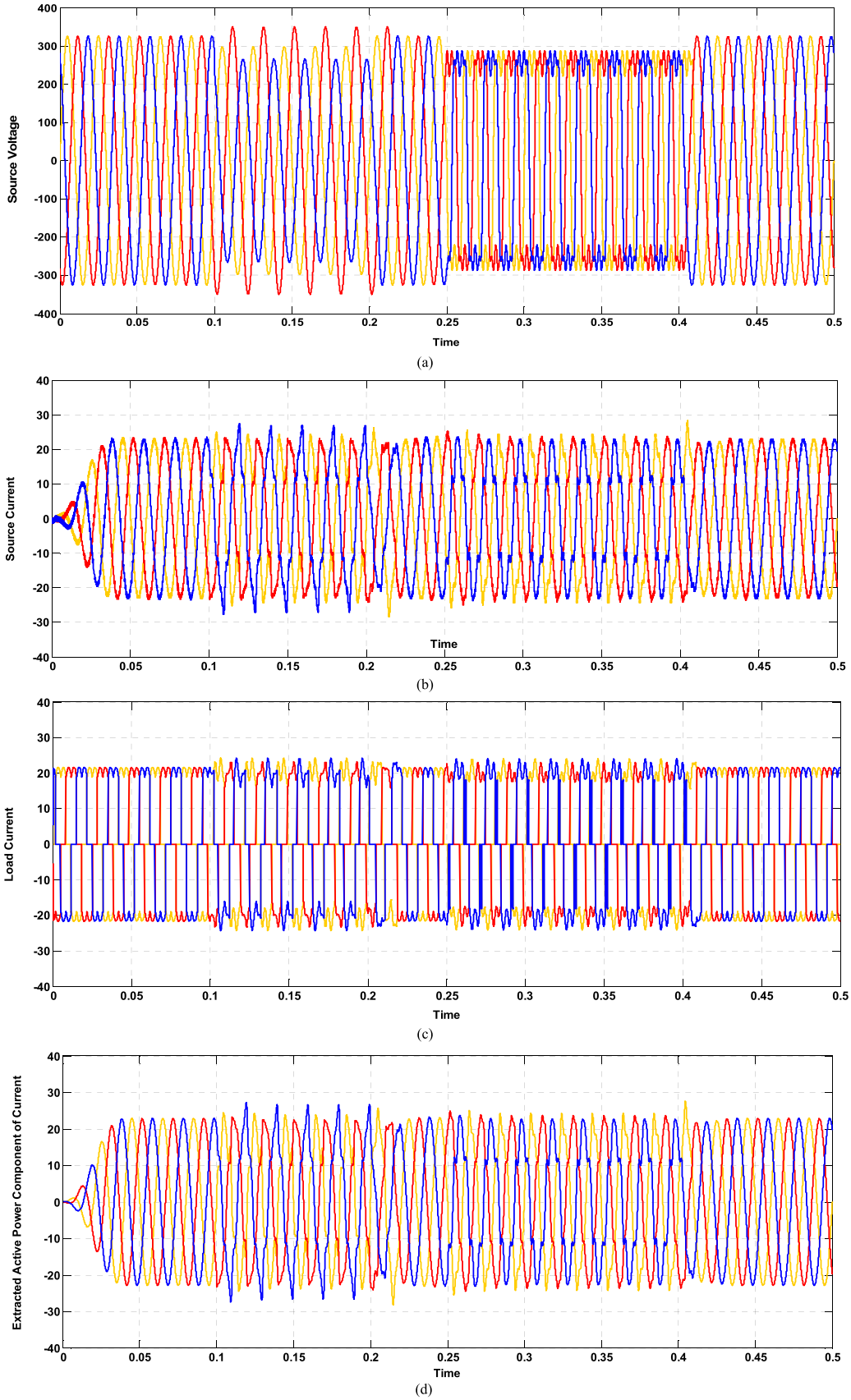

FIGURE 9. Dynamic performance of SAPF using p-q theory with an unbalanced or distorted source voltage.

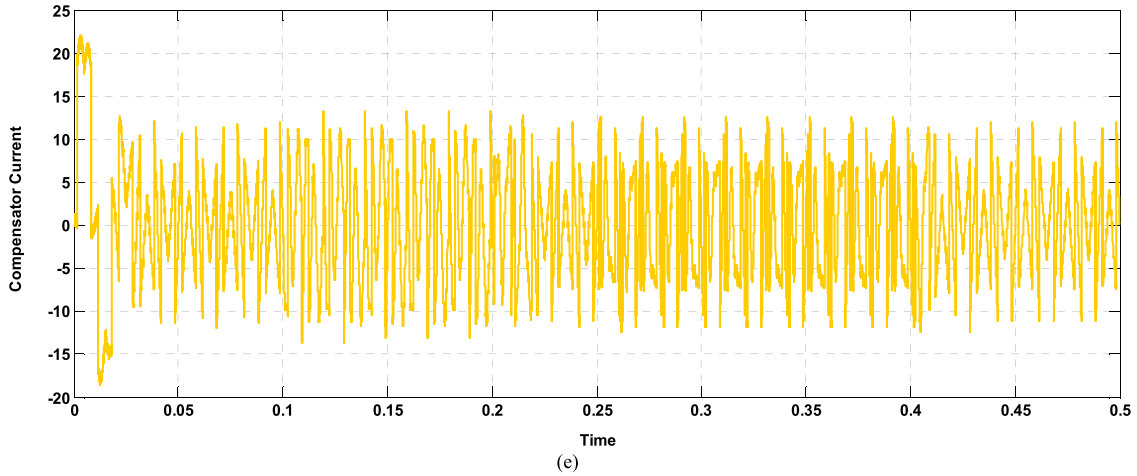

(e)

FIGURE 9. *(Continued.)* **Dynamic performance of SAPF using p-q theory with an unbalanced or distorted source voltage.**

The effectiveness of a control theory under source side impurity is very essential for the robust operation of the compensator. For simulation purpose, both distortions, as well as unbalance from the utility side, is assumed in the same system like that of Case-1. For the period, 0.1 to 0.20-second utility voltage is extremely unbalanced. For the period 0.25 to 0.40-second utility voltage is highly distorted. For the period, 0.0 to 0.1-second utility voltage is a fully fundamental and positive sequence one.

The waveforms of the p-q theory, SRF theory and Lyapunov function based controller are shown in figure 9, 10 and 11 respectively. The waveform of source voltage, source current, load current, reference current and compensation current are shown under each of the cases. Both p-q and SRF theory fail to detect the active power component of load current precisely during unbalance as well as distortion in the utility voltage and the reason being the SAPF fails to maintain the source current at purely sinusoidal. However, with the Lyapunov function based controller, the detected active power component of load current is closer to the actual one and sinusoidal as shown in figure 11(c).

Here is worth to mention again that under the wrong detection of reference current, SAPF becomes a source of disturbance itself. Accurate tracking of detected reference current by the injected compensation current is important but accurate detection of reference current by the control techniques is also equally important. The results obtained under the considered second case of system scenario clearly shows the effectiveness of the Lyapunov function based controller under the source side disturbances. Though the active filter's compensation effectiveness is not affected by utility side voltage distortion, as it happens with passive filtering, yet the control action of active technologies is still affected by such ill conditions.

The next target of the study is to assess the performance of the proposed Lyapunov function based controller by merging the scenario of case-1 with case-2. A large 13 bus standard IEEE DPS is undertaken for performance assessment and thereby naming the new scenario as case-3. Conceptually the PCC bears background unbalance because of loads connected at other buses. Therefore, case-3 gives challenges for SAPF to compensation harmonics under a large distribution instead of an approximated 2-bus system. Also a high voltage industrial load of nonlinear characteristics is considered in place of a three phase rectifier.

Figure 12(a) [41] shows the MATLAB/Simulink based model of modified IEEE 13 bus test distribution network with 3-phase chopper fed DC motor industrial drive and SAPF installed for compensation purpose while complete schematic of Lyapunov function based SAPF is depicted in figure 12(b). The parameters used in the simulation are specified by table 4. The parameters specified in table 4 includes motor load, distribution network and SAPF parameters. Also, the bus is also assumed fully fundamental positive sequence at 4.16 kV RMS line to line and free from any nonlinearity or unbalance. Accordingly, reference DC link voltage is taken as 7000 Volt. The value of the DC-link capacitor is taken as 453 μF. The associated constants of PI controller gains are selected by hit and trial and kept fixed at 2.4 and 0.9 respectively.

The different waveforms of the system under PQ theory-based SAPF, being connected at the drive carrying bus, are shown in figure 13 for the after compensation case. Figure 13 comprises three waveforms namely source voltage, source current, SAPF current, load current and the DC link voltage. The source voltage is basically not the background voltage but the voltage at the PCC itself. DC link voltage can be seen getting at a stable point after 0.1 sec. The voltage at the PCC can be seen as being almost balanced from waveform 13 even under the presence of unbalanced loads in the background. Figure 14 depicts the waveforms of SRF theory-based SAPF.

The waveforms of the Lyapunov function based control technique are shown in figure 15, for after compensation case,

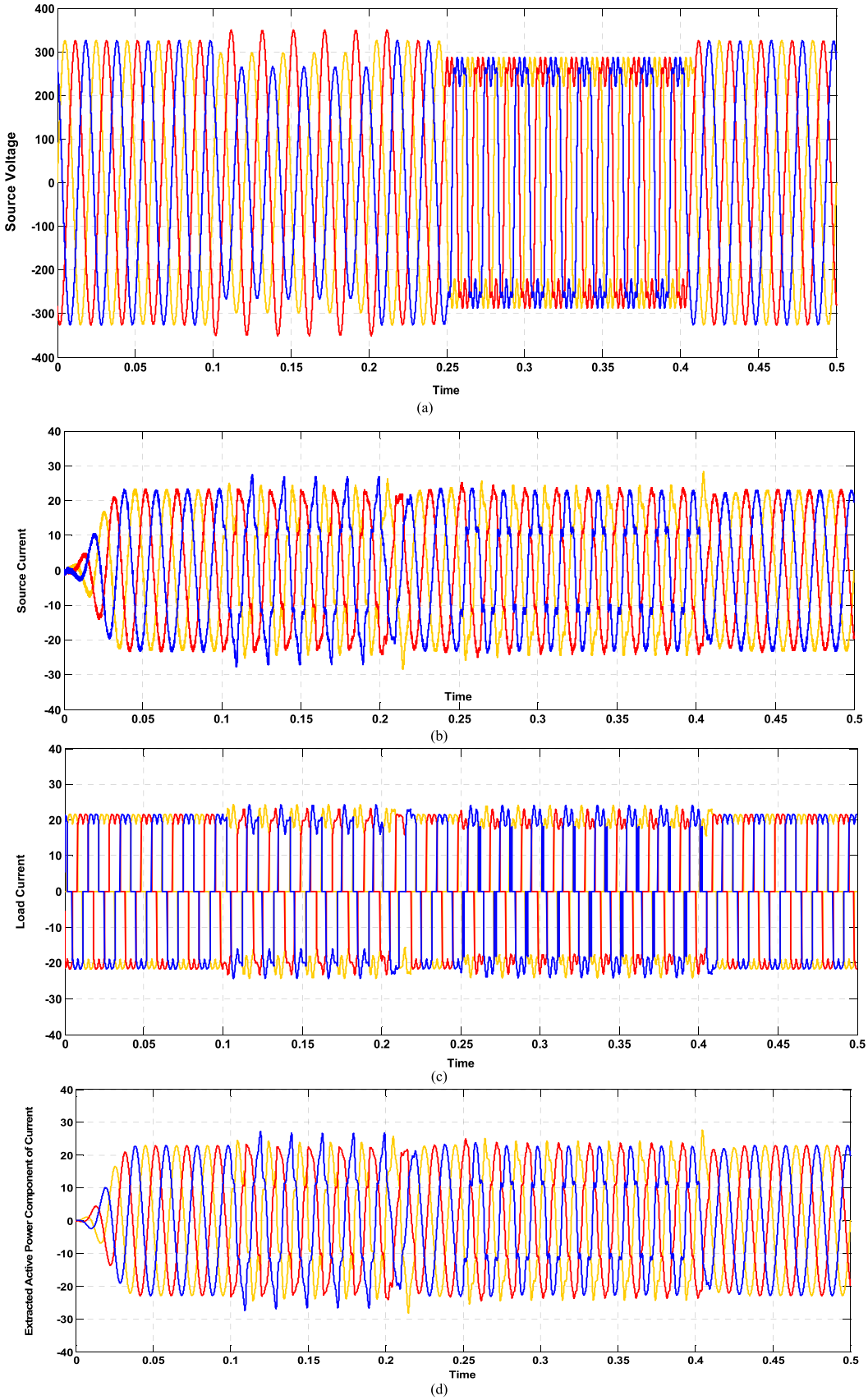

FIGURE 10. Dynamic performance of SAPF using SRF theory with an unbalanced or distorted source voltage.

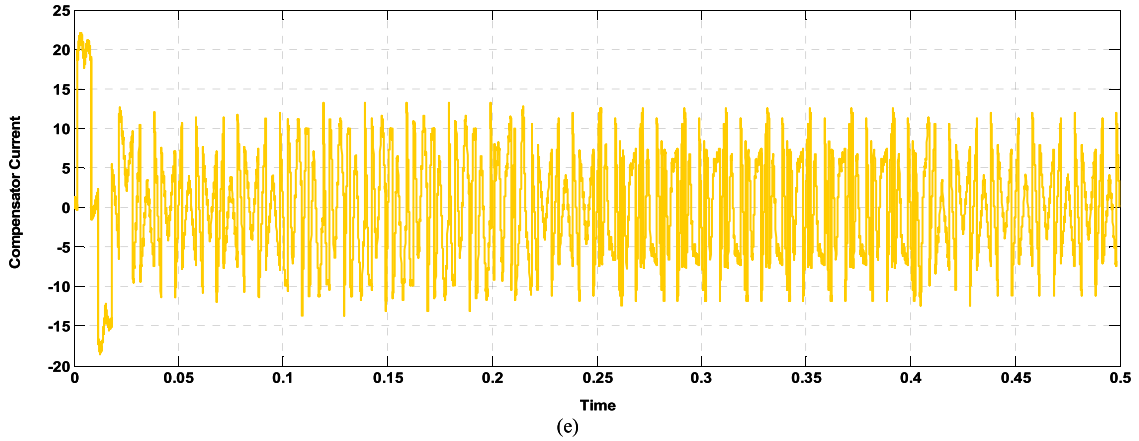

(e)

FIGURE 10. *(Continued.)* **Dynamic performance of SAPF using SRF theory with an unbalanced or distorted source voltage.**

TABLE 4. Specification parameters of the system.

Parameter	Value
Supply Voltage	4.16 kV (L-L), 50 Hz.
Feeder's Parameters	Per Ref. [39]
Load (Non-linear)	3-Phase Chopper Fed DC Motor Drive 200 HP, 380 V
DC-Capacitor	453 μF
Interfacing Inductor Values	L_f = 6.6 mH , R_f = 0.7 Ω
DC-link Reference Voltage	V_{dc} = 7000
PI-Controller's Parameters	K_p = 2.4, K_i = 0.9

TABLE 5. Comparative analysis of performance.

S. No.	Control Algorithm	% THD					
		Before Compensation			After Compensation		
		Phase A	Phase B	Phase C	Phase A	Phase B	Phase C
1.	IRP based Approach	29.18	30.04	28.25	4.57	4.69	4.25
2.	SRF Approach	29.18	30.04	28.25	4.88	4.76	4.65
3.	Lyapunov function Approach	29.18	30.04	28.25	1.59	1.61	1.52

with a modified IEEE 13 bus test distribution system loaded with 3-phase chopper fed DC motor drive. It can be seen from the waveforms of figure 15 that the Lyapunov function based control technique results in slightly better control of DC-link voltage hence offers enhanced performance in comparison to the other two techniques under discussion. Additionally, the impact of better DC link voltage control can be seen by the harmonic currents present in the source current also. Comparing the performance of the Lyapunov function based control technique with those widespread employed PQ and SRF theory, in the case of the large distribution system and industrial load, from figure 13, 14 and 15, indicates marginal improvement.

Comparative analysis of the performance of three techniques under discussion is shown in Table 5. The THD of source current by Lyapunov function based control technique is 1.59 % in phase a, 1.61 % in phase b, 1.52 % in phase c which is under the limit as per IEEE standard 519 and lower than that of obtained with other two techniques under discussion. THD analysis performed through the FFT tool of MATLAB/Simulink makes the better performance of the Lyapunov function based control technique evident also in the case of the large distribution system and industrial load.

The fourth and foremost scenario of the study is to perform the assessment of Lyapunov function based controller under high penetration of renewable energy in the grid. As mentioned in the introduction section also that penetration level of renewable energy cannot be enhanced of allowed to be more than a particular level because of deterioration of one or more performance indices with the penetration level being more than a particular one [42]. The harmonic performance of the system is one among the many crucial aspects that constraint the penetration level of renewable energy i.e. the concept of harmonic-constrained hosting capacity [43]. Figure 16 gives the idea of the hosting capacity concept as well as its enhancement by application of harmonic filtering [44].

The background performance of the system is the one that belongs to before integration of DG into the grid. The limiting performance is the one decided by the imposed IEEE Standards. Figure 16 shows how harmonic contamination increase in the system with an increase in the penetration level of renewable energy. One curve is associated without the presence of a harmonic compensator while the other assumes the compensation by the harmonic filter. The better the background performance of the system is the more amount of renewable energy can be injected into the system. The fact

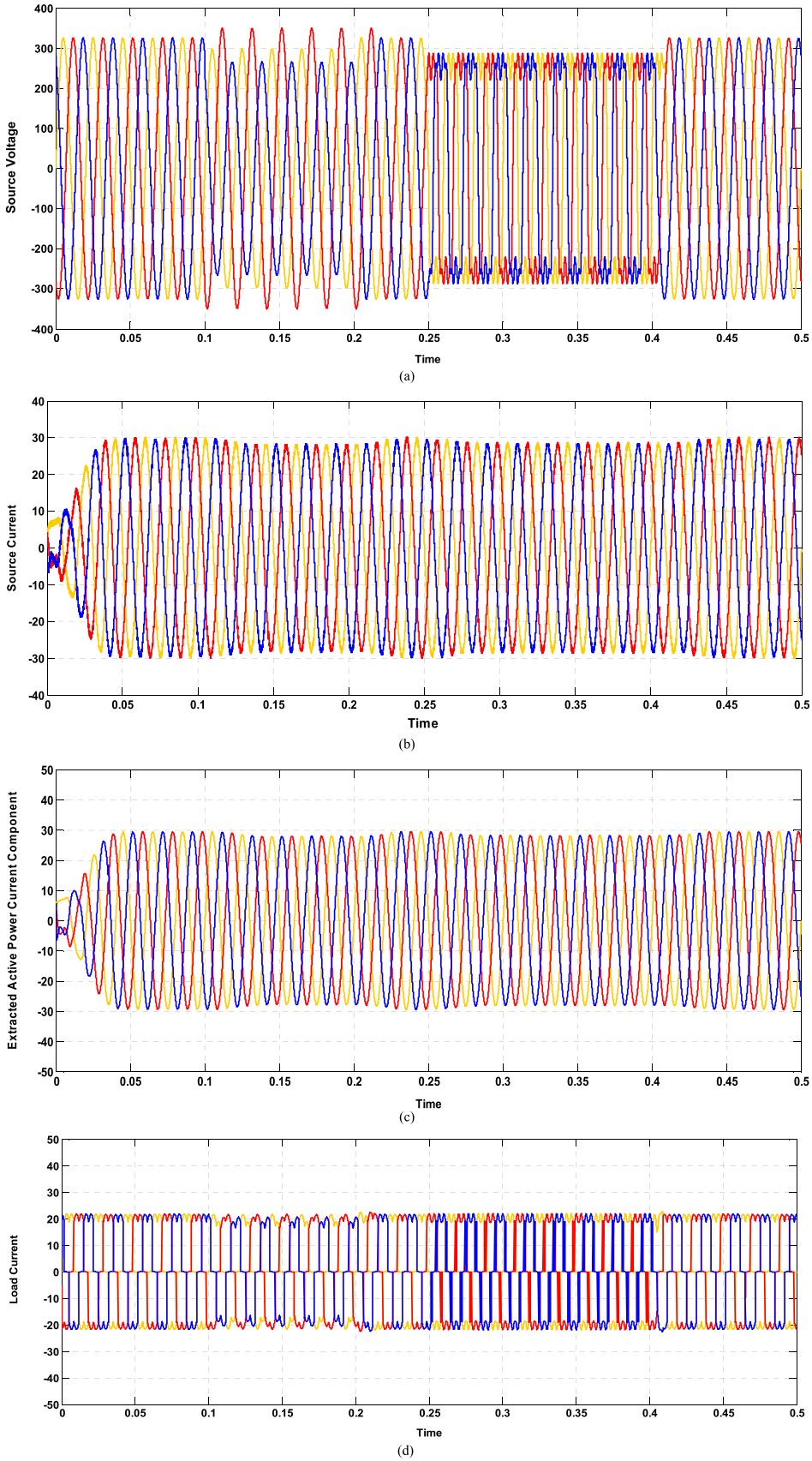

FIGURE 11. Dynamic performance of SAPF using Lyapunov function based controller with an unbalanced or distorted source voltage.

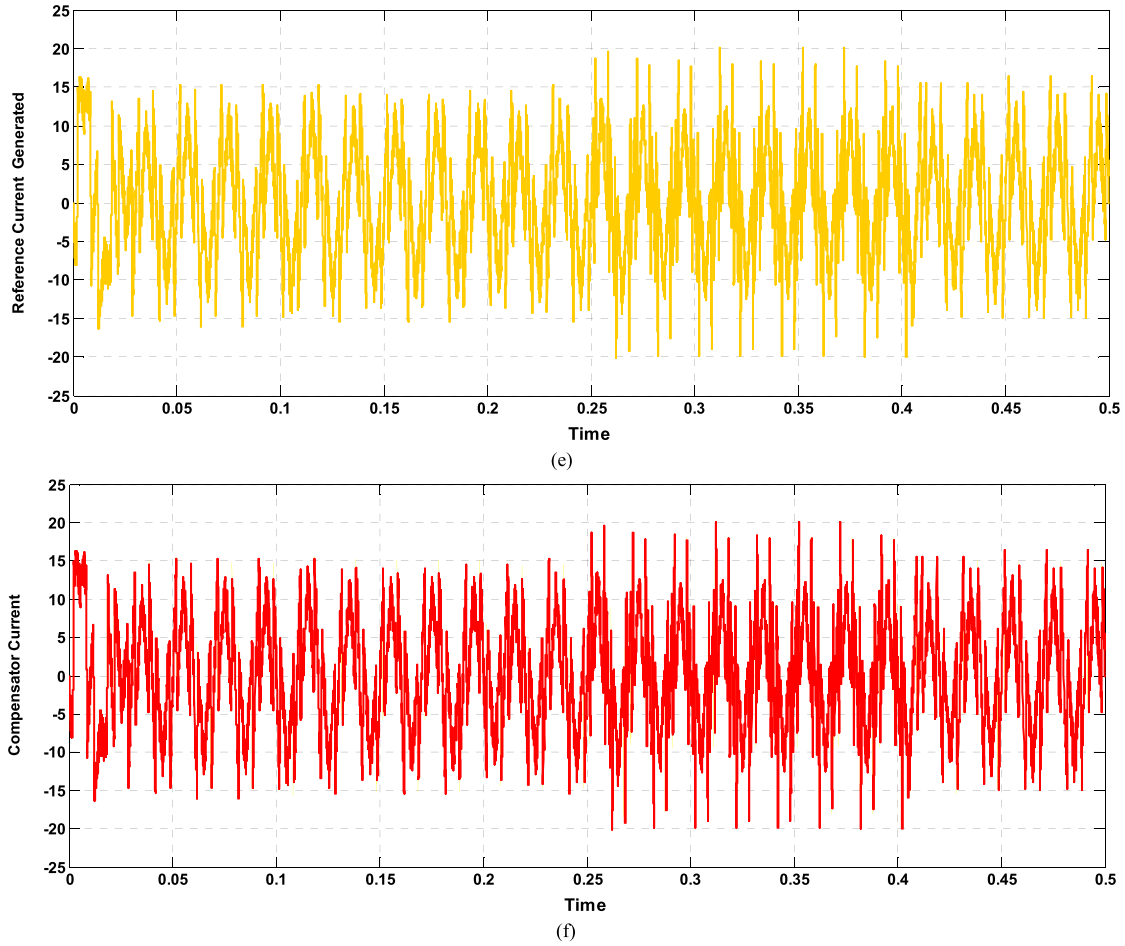

FIGURE 11. *(Continued.)* **Dynamic performance of SAPF using Lyapunov function based controller with an unbalanced or distorted source voltage.**

can be vindicated by the plots obtained for three PIs versus DG penetration level for typical DPS. Hence keeping the harmonic performance of the DPS at the best level can be the best practice to enable it to host high penetration of renewable energy. Therefore, harmonic compensators play an important role in doing the same. The better a harmonic compensation device does perform the more hosting capacity a system has. However, the parameter for determining the performance of the harmonic compensator can be anything such as its control algorithm, reference current detection technique or even the controller employed for DC-link voltage control. Hence to the author's knowledge, the HC-HC enhancement offered by a shunt active power filter can be a significant base for comparing their controller algorithm's performance. The same has been done by the authors in the last one out of the four considered system scenario.

The system taken under study is shown in figure 17. The entire system is simulated in MATLAB/Simulink. The fundamental frequency voltage of the utility grid or so-called source is 3-phase balanced and has an RMS line-line rating of 11 kV at a frequency of 50 Hz. The distribution feeder is fully three phases transposed and has fundamental frequency resistance and inductive reactance of 0.455 Ω and 1.165 Ω respectively. All the simulations are performed by taking base voltage of 11 kV and base MVA of 10 MVA in the Simulink model. The nature of the load is assumed to be hybrid i.e. the combination of linear and nonlinear

TABLE 6. Harmonic contents of nonlinear load.

Harmonic Order	Magnitude (%)	Phase (Degree)
1	100	-9.2
5	76.14	132.9
7	56.87	-67.6
11	20.38	59.2
13	9.48	189.1
17	7.42	241.6
19	6.26	22.7
23	2.99	93.6
25	3.02	213.2
29	2.31	-57.4
31	1.73	65.6
35	1.66	133.3
37	1.45	267.3
41	1.03	-26.6
43	1.05	99.5
47	0.82	181
49	0.72	-57.8

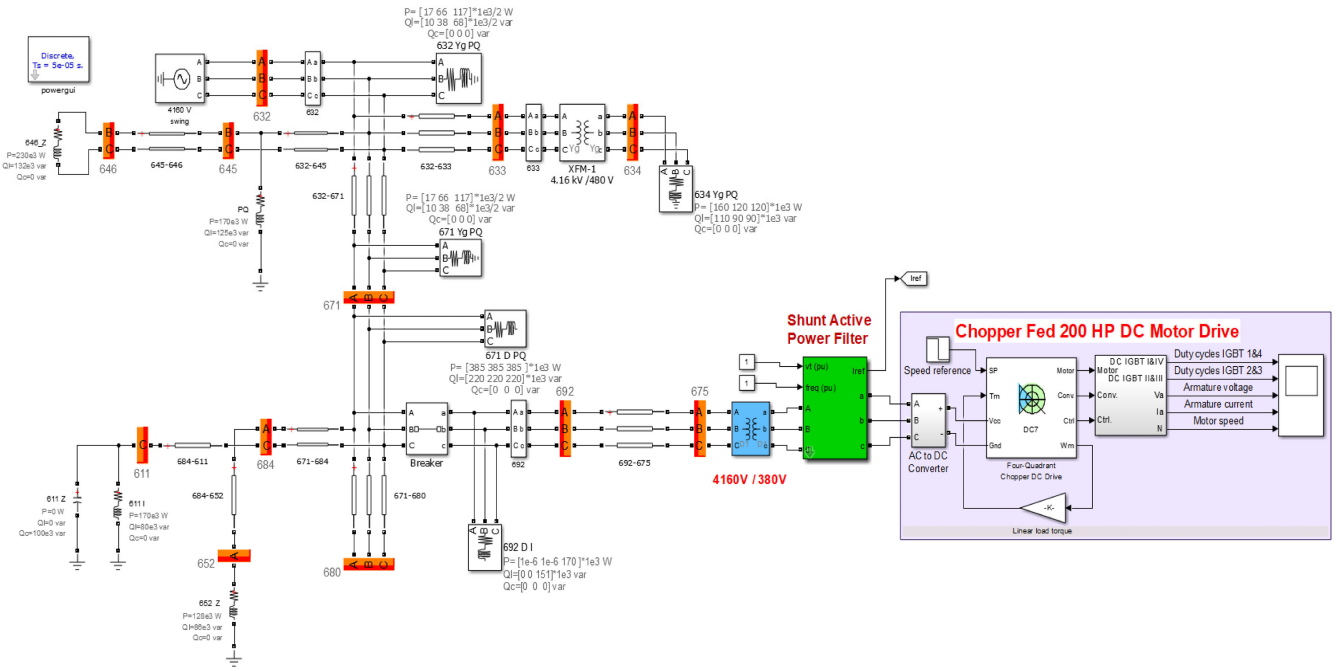

(a)

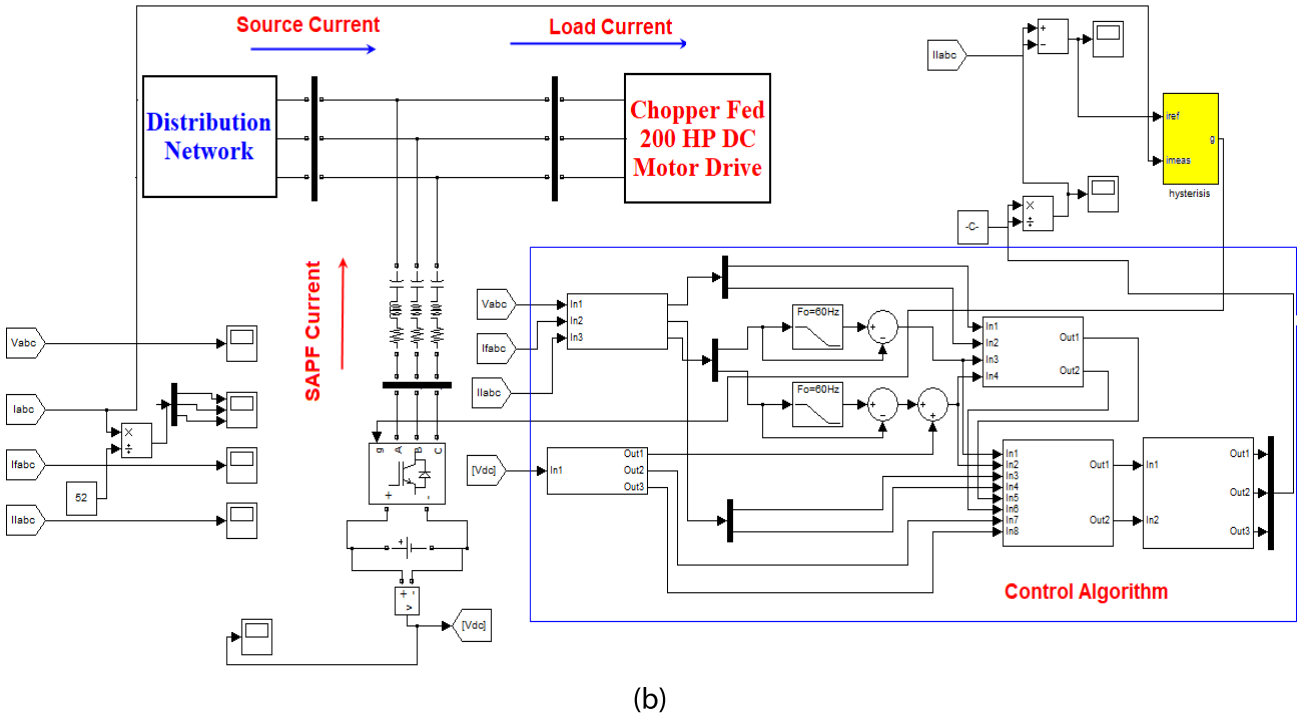

(b)

FIGURE 12. (a) Matlab/Simulink based model of modified IEEE 13 bus test distribution network with industrial motor drive and SAPF. (b) Complete schematic of Lyapunov function based SAPF.

loads. For simulation purpose, a PWM controlled 3-phase IM-drive is made to functions as a nonlinear load while a three-phase balanced RL-load works as a linear load. Total active power consumption by the hybrid load is 7.2 MW while total reactive power consumption is 3.8 MVAr. NLL is considered 25 % which means active and reactive power consumption by the linear load are 5.4 MW and 2.85 MVAR respectively and active and reactive power consumption by the nonlinear load are 1.8 MW and 0.95 MVAR respectively. The harmonic contents, obtained from the FFT analysis of the current drawn by the nonlinear load, are shown in table no. 6.

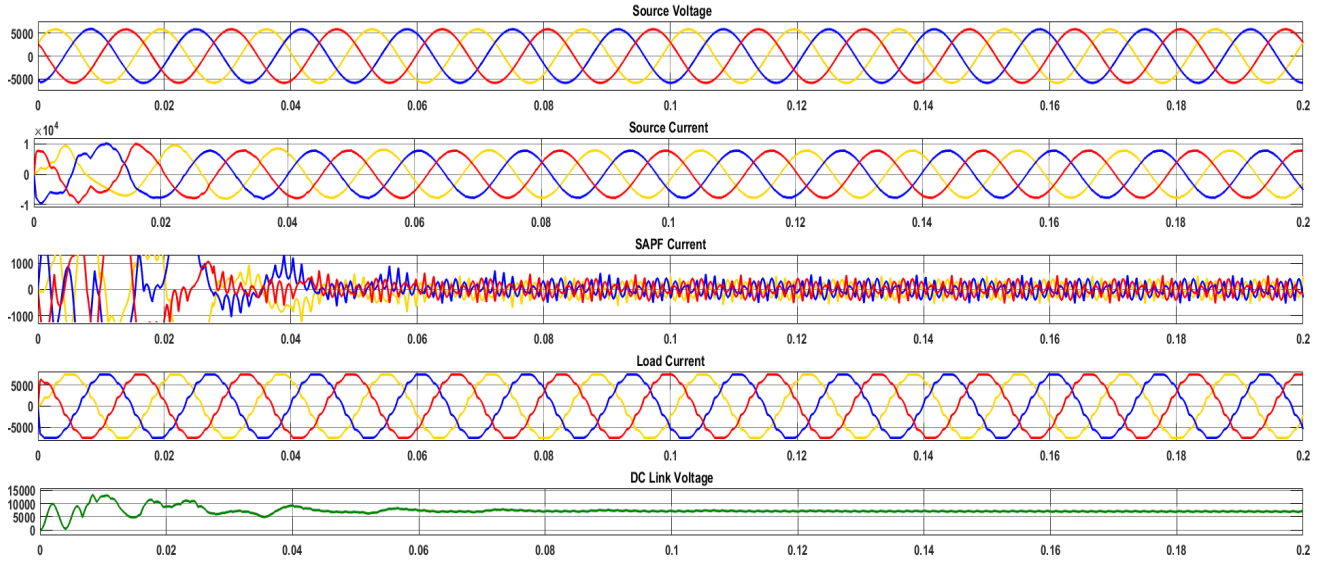

FIGURE 13. Waveforms of PQ theory-based SAPF after compensation.

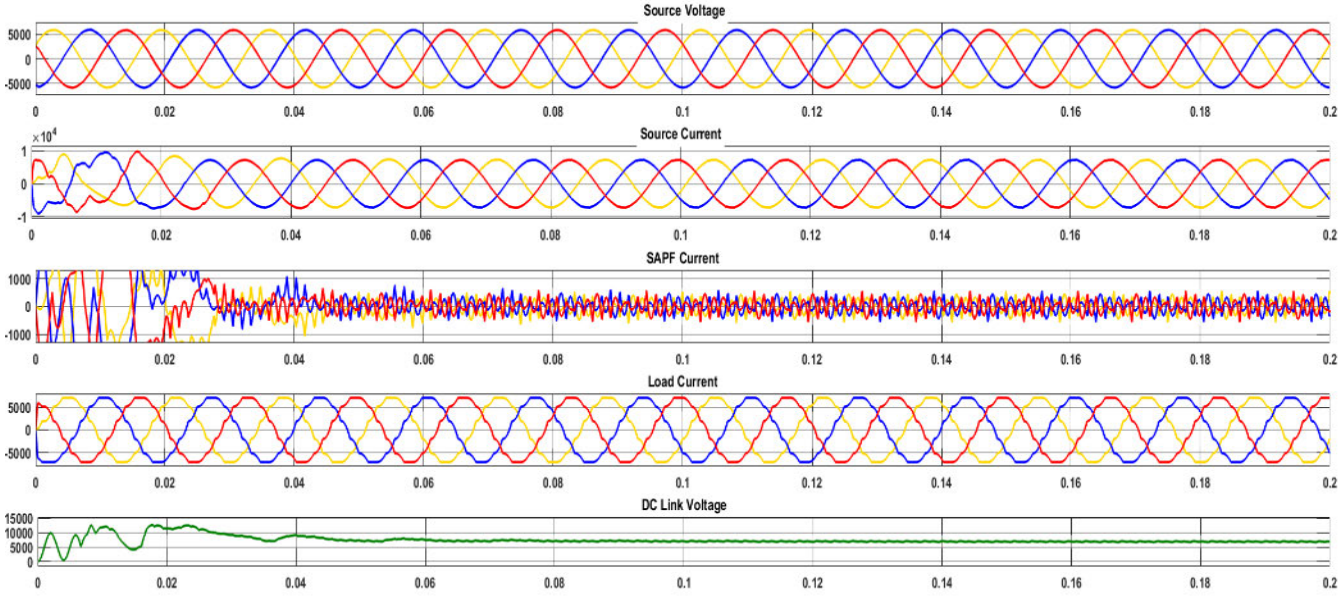

FIGURE 14. Waveforms of SRF theory-based SAPF after compensation.

Table no. 7 shows the performance comparison of the system under three cases in contrast to the uncompensated one. The uncompensated system can be observed to be having hosting capacity limited to 30.16%. The plots of performance indices versus DG penetration in uncompensated system are depicted in figure 19. The plots of five lower order harmonics in the line current with respect to DG penetration level clearly shows that 3rd order harmonics constraints the HC of the system to 30.16%. The resulted TDD in the source current is 5.54% and 3.67% is the voltage THD at PCC. The plots of performance indices versus DG penetration in the system with SAPF based on three theories are depicted in figure 20, 21 and 22 respectively.

It becomes clear from the three figures that the hosting capacity of the considered DPS gets boosted up to 60.98% owing to the harmonic compensation provided by SAPF based on the Lyapunov function controller. While the same is limited to 54.87% and 55.35% respectively in the case of p-q theory and SRF theory-based SAPF. The THD in source current, as well as voltage, is also minimum at 2.59% and 1.83% in the case of Lyapunov function based SAPF which is relatively lower with respect to the uncompensated system as

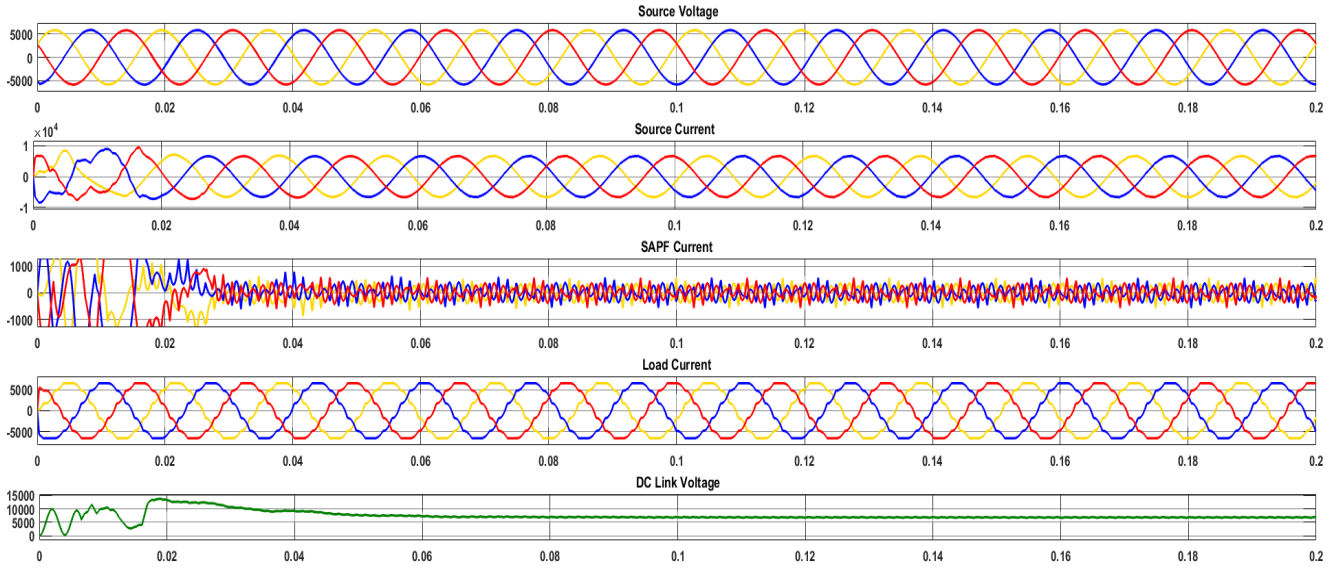

FIGURE 15. Waveforms of Lyapunov function based SAPF after compensation.

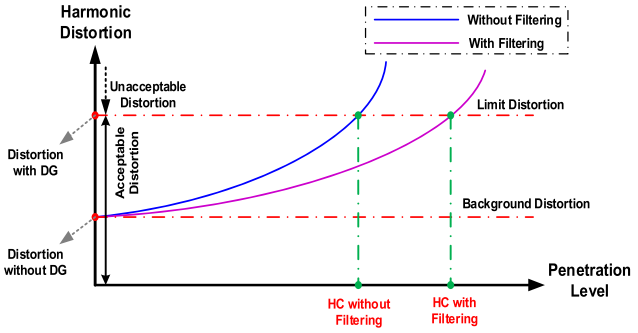

FIGURE 16. The idea of hosting capacity enhancement using harmonic filtering [44].

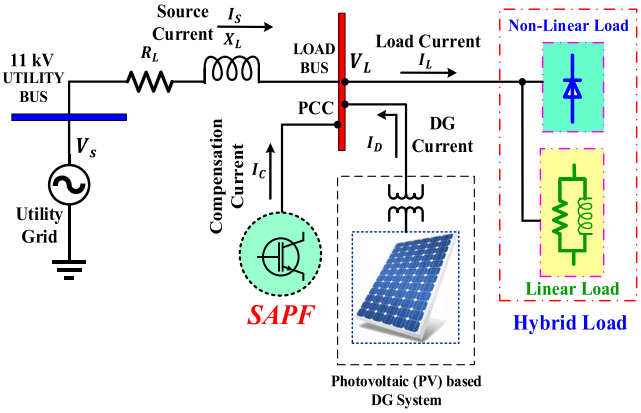

FIGURE 17. The configuration of the system under study.

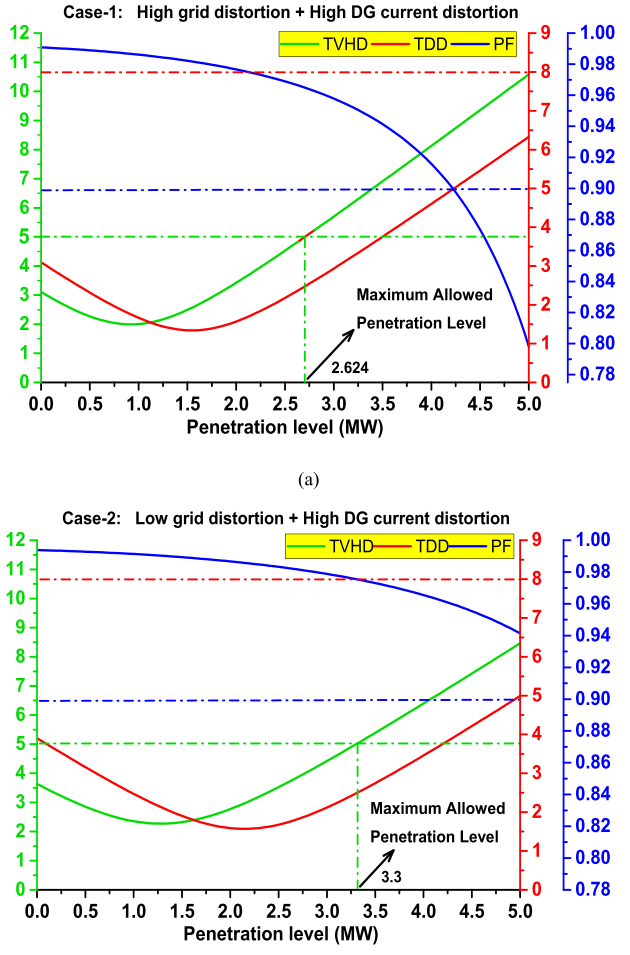

FIGURE 18. The impacts of DG penetration on three PQ indices.

well as adhered to the IEEE Std. 519. The economic, as well as technical benefits of high penetration of renewable energy, can also be seen in table 7. Total transmission losses of the system reduce from 165 kW to 22.98 kW and the voltage profile enhances from 0.9405 PU to 1.0009 PU. Though both categories of advantages include also the contribution of reactive power support provided by SAPF. Percentage HDF in the table, as well as the plots, stands for the harmonic de-rating factor that quantifies the ampacity of the distribution feeder

TABLE 7. Performance comparison of the system under three cases.

Parameter	Uncompensated System	Compensated System		
		P-Q Theory	SRF Theory	Lyapunov Function Based Theory
Voltage at the PCC (pu)	0.9405	1.0011	1.0009	1.0009
HDF of the distribution line (%)	99.28	98.97	99.01	98.77
TVHD at the PCC (%)	3.67	2.27	1.85	1.83
THD/TDD of the line current (%)	5.54	2.89	2.85	2.59
Transmission losses (kW)	165.00	34.19	33.18	22.98
PF at the PCC	0.7641	0.9100	0.9108	0.9100
MVA level of DG (MVA)	2.46	4.4761	4.5137	4.9694
DG-Power factor	0.9941	0.9945	0.9951	0.9957
Penetration level (MW)	2.45	4.4675	4.5069	4.9648
Hosting Capacity (%)	30.16	54.87	55.35	60.98

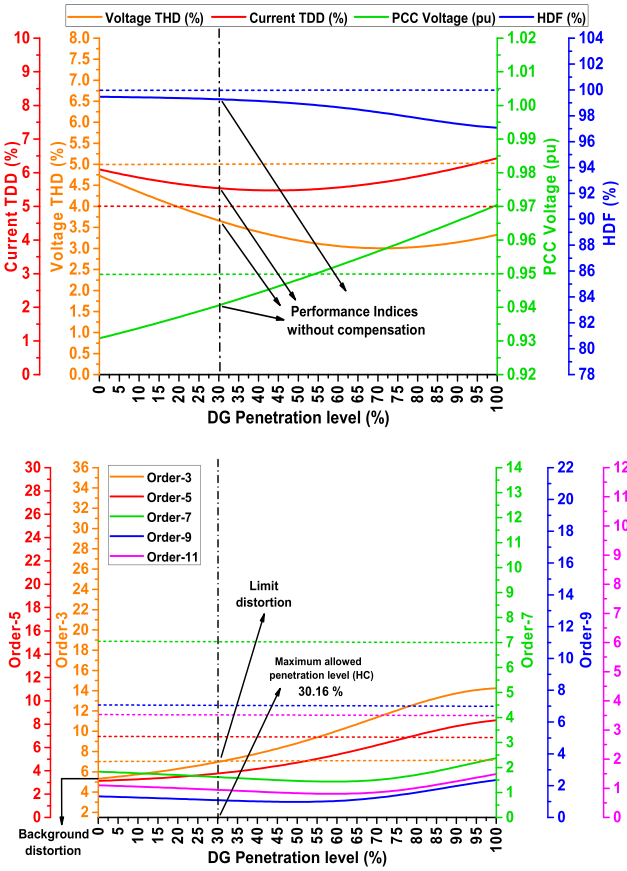

FIGURE 19. Performance indices versus DG penetration in uncompensated system.

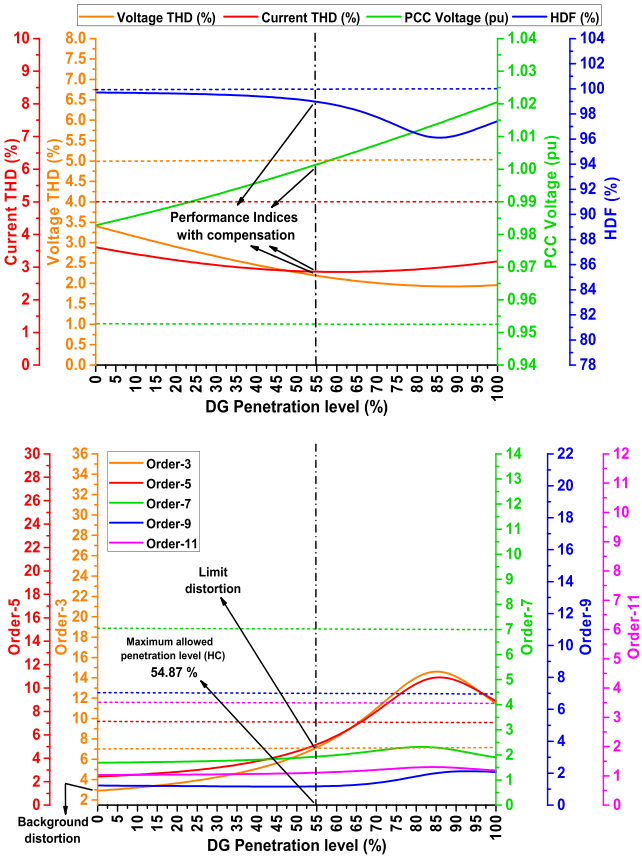

FIGURE 20. Performance indices versus DG penetration with p-q theory-based SAPF.

or cable in the harmonically contaminated environment. The same index has a threshold value of 100%. It can be clearly observed that HDF in the case of Lyapunov function based SAPF is minimum with 98.77% in contrast to the other two cases. The power factor is also improved by up to 91% in comparison to the power factor of 76.41% in the uncompensated system. The study therefore demonstrates the capability of the proposed Lyapunov function-based SAPF in

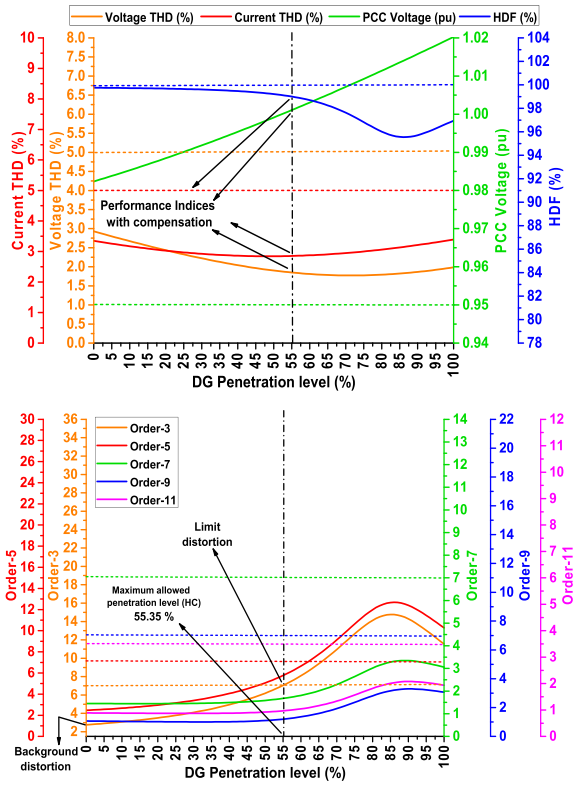

FIGURE 21. Performance indices versus DG penetration with SRF theory-based SAPF.

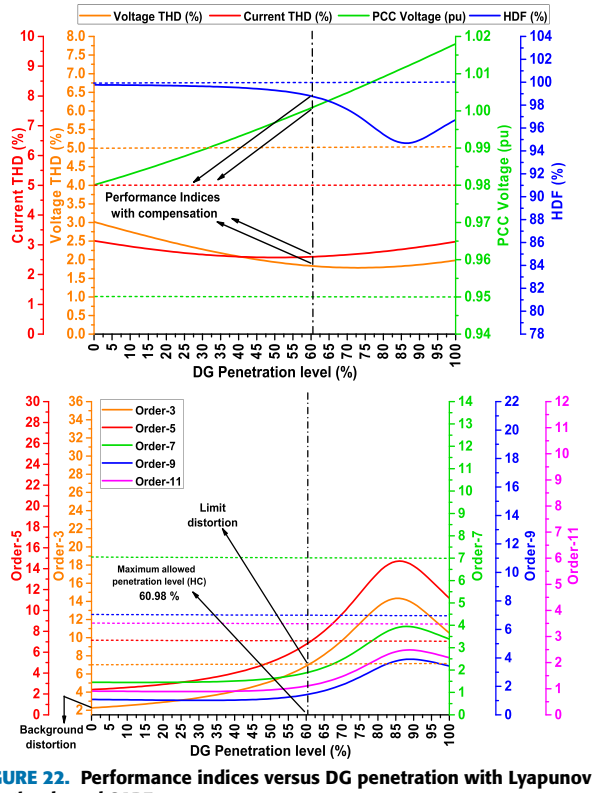

FIGURE 22. Performance indices versus DG penetration with Lyapunov function based SAPF.

not only reducing harmonic distortion in the DPS but also its potential of increasing the maximum permissible penetration level of renewable energy and therefore its offered benefits.

VI. CONCLUSION

A control algorithm, based on the Lyapunov function, is proposed for SAPF to mitigate harmonics and reactive power compensation of nonlinear loads. The performance of SAPF has been found satisfactory under all four cases of the study. The control algorithm is established on the Lyapunov function for achieving global stability in the system. The simulation results validate the control approach for SAPF. A hysteresis controller has been used to generate a switching signal for the voltage source inverter. Based on simulation results following conclusions have been drawn.

1) All the control algorithm's (p-q theory, SRF theory, Lyapunov function based control theory) performance found satisfactory i.e. THD is less than 5% according to IEEE 519 standards.
2) Under the fully fundamental plus balanced source voltage and purely nonlinear loading condition Lyapunov function-based control algorithm gives the best performance over the other two control algorithms which are commonly used.
3) The THD of the source current under the Lyapunov function based control algorithm is 1.61% in phase a, 2.33% in phase b, 1.99% in phase c when applied on a two-bus system under purely nonlinear load. In the case of a modified 13-bus system, the same with Lyapunov function based control algorithm is 1.59% in phase a, 1.61% in phase b, 1.52% in phase c.
4) In case of distortion and unbalance present in the utility's voltage, the detection of the reference current is accurately performed by the Lyapunov function-based control algorithm and superiorly in contract to the other two control algorithms.
5) It is also inferred that the dynamic response of the system with the Lyapunov function-based control algorithm to be better than the other two control algorithms.
6) Last but not the least, the harmonic and reactive power compensation offered by Lyapunov function-based SAPF is better also in the case of renewable energy's penetration. The proposed theory-based SAPF has the potential of enhancing the penetration level of HC-HC of the modern and polluted DPS up to more extent.

REFERENCES

[1] X. Zong, P. A. Gray, and P. W. Lehn, "New metric recommended for IEEE standard 1547 to limit harmonics injected into distorted grids," *IEEE Trans. Power Del.*, vol. 31, no. 3, pp. 963–972, Jun. 2016.
[2] O. F. Kececioglu, H. Acikgoz, C. Yildiz, A. Gani, and M. Sekkeli, "Power quality improvement using hybrid passive filter configuration for wind energy systems," *J. Electr. Eng. Technol.*, vol. 12, no. 1, pp. 207–216, Jan. 2017.
[3] G. K. Singh, "Power system harmonics research: A survey," *Eur. Trans. Electr. Power*, vol. 19, no. 2, pp. 151–172, Mar. 2009.
[4] S. S. Reddy and P. R. Bijwe, "Real time economic dispatch considering renewable energy resources," *Renew. Energy*, vol. 83, pp. 1215–1226, Nov. 2015.
[5] *IEEE Recommended Practice and Requirements for Harmonic Control in Electric Power Systems*, IEEE Std 519-2014 (Revision IEEE Std 519-1992), Nov. 2014, pp. 1–29.

[6] *IEEE Standard for Interconnection and Interoperability of Distributed Energy Resources With Associated Electric Power Systems Interfaces*, IEEE Std 1547-2018 (Revision of IEEE Std 1547-2003), Institute of Electrical and Electronics Engineers, Jun. 2018.

[7] S. S. Reddy, A. R. Abhyankar, and P. R. Bijwe, "Co-optimization of energy and demand-side reserves in day-ahead electricity markets," *Int. J. Emerg. Electr. Power Syst.*, vol. 16, no. 2, pp. 195–206, Apr. 2015.

[8] I. N. Santos, M. H. J. Bollen, and P. F. Ribeiro, "Exploring the concept of hosting capacity for harmonic distortions assessment," in *Proc. IEEE Power Energy Soc. Gen. Meeting*, Jul. 2015, pp. 1–5.

[9] S. M. Ismael, S. H. E. A. Aleem, A. Y. Abdelaziz, and A. F. Zobaa, "State-of-the-art of hosting capacity in modern power systems with distributed generation," *Renew. Energy*, vol. 130, pp. 1002–1020, Jan. 2019.

[10] M. Bajaj, S. Rautela, and A. Sharma, "A comparative analysis of control techniques of SAPF under source side disturbance," in *Proc. Int. Conf. Circuit, Power Comput. Technol. (ICCPCT)*, Mar. 2016, pp. 1–7.

[11] A. Singh Rana, M. Bajaj, and S. Gairola, "Optimal power flow solution in smart grid environment using SVC and TCSC," in *Advanced Communication and Control Methods for Future Smartgrids*. New York, NY, USA: IntechOpen, 2019, pp. 1–22.

[12] M. Bajaj, V. K. Dwivedi, A. Kumar, and A. Bansal, "Design and simulation of DSTATCOM for power quality enhancement in distribution networks under various fault condition," *Int. J. Emerg. Technol. Adv. Eng.*, vol. 3, no. 4, pp. 620–626, 2013.

[13] R. Singh, A. K. Singh, A. Gupta, and A. K. Singh, "An improved approach for control of a grid connected wind farms and its STATCOM based stability analysis," in *Proc. IEEE Int. Conf. Signal Process., Comput. Control*, Mar. 2012, pp. 1–4.

[14] M. Bajaj and A. S. Rana, "Harmonics and reactive power compensation of three phase induction motor drive by photovoltaic-based DSTATCOM," *Smart Sci.*, vol. 6, no. 4, pp. 319–329, Oct. 2018.

[15] M. Bajaj, "Design and simulation of hybrid DG system fed single-phase dynamic voltage restorer for smart grid application," *Smart Sci.*, vol. 8, pp. 24–38, Apr. 2020.

[16] S. B. Singh, A. K. Singh, and P. Thakur, "Assessment of induction motor performance under voltage unbalance condition," in *Proc. IEEE 15th Int. Conf. Harmon. Qual. Power*, Jun. 2012, pp. 256–261.

[17] M. Bajaj and A. K. Singh, "Grid integrated renewable DG systems: A review of power quality challenges and state-of-the-art mitigation techniques," *Int. J. Energy Res.*, vol. 44, no. 1, pp. 26–69, Jan. 2020.

[18] J. A. Momoh, S. S. Reddy, and Y. Baxi, "Stochastic Voltage/Var control with load variation," in *Proc. IEEE PES Gen. Meeting | Conf. Expo.*, Jul. 2014, pp. 1–5.

[19] M. Bajaj, N. K. Sharma, M. Pushkarna, H. Malik, M. A. Alotaibi, and A. Almutairi, "Optimal design of passive power filter using multi-objective Pareto-based firefly algorithm and analysis under background and load-side's nonlinearity," *IEEE Access*, vol. 9, pp. 22724–22744, 2021.

[20] M. Bajaj and A. K. Singh, "Designing of a solar energy based single phase dynamic voltage restorer using fuzzy logic controlled novel boost inverter," in *Proc. IEEE 9th Power India Int. Conf. (PIICON)*, Feb. 2020, pp. 1–6.

[21] M. Bajaj, C. Bhardwaj, and M. Pushkarna, "A comparative study of control techniques of distribution-STATCOM under abnormal source voltage," in *Proc. 2nd Int. Conf. Adv. Electr., Electron., Inf., Commun. Bio-Inform. (AEEICB)*, Feb. 2016, pp. 166–171.

[22] M. Bajaj and M. Pushkarna, "An IRP based control algorithm for load compensation by DSTATCOM under polluted supply system," in *Proc. Int. Conf. Control Commun. Comput. India (ICCC)*, Nov. 2015, pp. 303–308.

[23] M. Bajaj, M. Pushkarna, A. S. Rana, and M. T. Khan, "A modified algorithm for time varying reactive power control and harmonics compensation by D-STATCOM," in *Proc. Annu. IEEE India Conf. (INDICON)*, Dec. 2015, pp. 1–5.

[24] A. Kumar, V. K. Dwivedi, S. Maity, and M. Bajaj, "Performance comparison of control algorithms for load compensation using D-STATCOM under abnormal source voltage," *J. Autom. Control Eng.*, vol. 2, no. 1, pp. 54–58, 2014.

[25] Y. K. and A. N. Akagi, "Generalized theory of the instantaneous reactive power in three-phase circuits," in *Proc. IEEE IPEC*, 1983, pp. 821–827.

[26] S. Bhattacharya, D. M. Divan, and B. Banerjee, "Synchronous frame harmonic isolator using active series filter," in *Proc. Eur. Power Electron. Conf.*, 1991, pp. 3030–3035.

[27] M. Aredes and E. H. Watanabe, "New control algorithms for series and shunt three-phase four-wire active power filters," *IEEE Trans. Power Del.*, vol. 10, no. 3, pp. 1649–1656, Jul. 1995.

[28] M. Karimi-Ghartemani and M. Iravani, "A nonlinear adaptive filter for online signal analysis in power systems: Applications," *IEEE Trans. Power Del.*, vol. 17, no. 2, pp. 617–622, Apr. 2002.

[29] L. P. Kunjumuhammed and M. K. Mishra, "A control algorithm for single-phase active power filter under non-stiff voltage source," *IEEE Trans. Power Electron.*, vol. 21, no. 3, pp. 822–825, May 2006.

[30] M. Mishra and P. Linash, "A fast transient response single phase active power filter," in *Proc. TENCON-IEEE Region 10th Conf.*, Nov. 2005, pp. 1–6.

[31] B. Singh, V. Verma, and J. Solanki, "Neural network-based selective compensation of current quality problems in distribution system," *IEEE Trans. Ind. Electron.*, vol. 54, no. 1, pp. 53–60, Feb. 2007.

[32] G. Bhuvaneswari and M. G. Nair, "Design, simulation, and analog circuit implementation of a three-phase shunt active filter using the I_{cos} Φ algorithm," *IEEE Trans. Power Del.*, vol. 23, no. 2, pp. 1222–1235, Apr. 2008.

[33] H. Komurcugil and O. Kukrer, "A new control strategy for single-phase shunt active power filters using a Lyapunov function," *IEEE Trans. Ind. Electron.*, vol. 53, no. 1, pp. 305–312, Feb. 2006.

[34] S. Rahmani, A. Hamadi, and K. Al-Haddad, "A Lyapunov-function-based control for a three-phase shunt hybrid active filter," *IEEE Trans. Ind. Electron.*, vol. 59, no. 3, pp. 1418–1429, Mar. 2012.

[35] B. Sourabh, "Applications of DSTATCOM using MATLAB/simulation in power system," *Res. J. Recent Sci.*, vol. 1, no. 1, pp. 430–433, 2012.

[36] B. Singh and S. Arya, "Design and control of a DSTATCOM for power quality improvement using cross correlation function approach," *Int. J. Eng., Sci. Technol.*, vol. 4, no. 1, pp. 74–86, Dec. 2012.

[37] V. Mahajan, P. Agarwal, and H. O. Gupta, "Simulation of shunt active power filter using instantaneous power theory," in *Proc. IEEE 5th Power India Conf.*, Dec. 2012, pp. 1–5.

[38] M. Bajaj and A. K. Singh, "An analytic hierarchy process-based novel approach for benchmarking the power quality performance of grid-integrated renewable energy systems," *Electr. Eng.*, vol. 102, no. 3, pp. 1153–1173, Sep. 2020.

[39] V. Dinavahi, M. Iravani, and R. Bonert, "Real-time digital simulation and experimental verification of a D-STATCOM interfaced with a digital controller," *Int. J. Electr. Power Energy Syst.*, vol. 26, no. 9, pp. 703–713, Nov. 2004.

[40] P. K. Madaria, M. Bajaj, S. Aggarwal, and A. K. Singh, "A grid-connected solar PV module with autonomous power management," in *Proc. IEEE 9th Power India Int. Conf. (PIICON)*, Feb. 2020, pp. 1–6.

[41] M. Bajaj, A. K. Singh, M. Alowaidi, N. K. Sharma, S. K. Sharma, and S. Mishra, "Power quality assessment of distorted distribution networks incorporating renewable distributed generation systems based on the analytic hierarchy process," *IEEE Access*, vol. 8, pp. 145713–145737, 2020.

[42] Y. Naderi, S. H. Hosseini, S. Ghassem Zadeh, B. Mohammadi-Ivatloo, J. C. Vasquez, and J. M. Guerrero, "An overview of power quality enhancement techniques applied to distributed generation in electrical distribution networks," *Renew. Sustain. Energy Rev.*, vol. 93, pp. 201–214, Oct. 2018.

[43] M. Bajaj and A. K. Singh, "A streamlined approach for assessing the power quality in renewable energy systems," in *Proc. IEEE 17th India Council Int. Conf. (INDICON)*, Dec. 2020, pp. 1–6.

[44] M. Bajaj and A. K. Singh, "Hosting capacity enhancement of renewable-based distributed generation in harmonically polluted distribution systems using passive harmonic filtering," *Sustain. Energy Technol. Assessments*, vol. 44, Apr. 2021, Art. no. 101030.

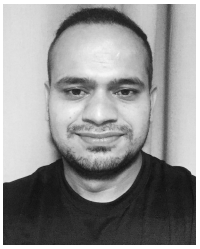

MOHIT BAJAJ (Member, IEEE) was born in Roorkee, India, in 1988. He received the bachelor's degree in electrical engineering from the FET, Gurukula Kangri Vishwavidhyalya, Haridwar, India, in 2010, and the M.Tech. degree in power electronics and ASIC design from NIT Allahabad, India, in 2013. He is currently pursuing the Ph.D. degree with the Department of Electrical and Electronics Engineering, NIT Delhi, India. He has academic experience of five years. He has published over 30 research articles in reputed journals, international conferences, and book chapters. His research interests include power quality improvement in renewable DG systems, distributed generations planning, application of multi-criteria decision making in power systems, custom power devices, and the IoT and smart grids. He is a member of PES.

AYMEN FLAH was born in Gabès, Tunisia, in 1983. He received the bachelor's degree in electrical engineering and the M.Tech. degree from the ENIG, Tunisia, in 2007 and 2009, respectively, and the Ph.D. degree from the Department of Electrical Engineering, in 2012. He has academic experience of 11 years. He has published over 40 research articles in reputed journals, international conferences, and book chapters. His research interests include electric vehicle, power systems, and renewable energy.

MAJED ALOWAIDI (Member, IEEE) received the B.Eng. degree (Hons.) from the Riyadh College of Technology, in 2006, and the M.A.S. and Ph.D. degrees in computer engineering from the University of Ottawa, in 2012 and 2018, respectively. He is currently working as an Assistant Professor and the Head of IT Department, College of Computer and Information Science, Majmaah University, Majmaah, Saudi Arabia. Since 2012, he has been a member of MCRLAB, University of Ottawa, Canada. His research interests include cybersecurity, the IoT, semantic Web, cloud and edge computing, and smart city.

NAVEEN KUMAR SHARMA (Senior Member, IEEE) received the B.Tech. degree in electrical and electronics engineering from Uttar Pradesh Technical University, Lucknow, in 2008, the M.Tech. and Ph.D. degrees in power system from the National Institute of Technology Hamirpur (H.P.), India, in 2010 and 2014, respectively. He worked as a Lecturer with the Department of Electrical Engineering, National Institute of Technology Hamirpur (H.P.), from March 2014 to May 2017. He is an Assistant Professor with the Department of Electrical Engineering, I. K. Gujral Punjab Technical University Main Campus, Kapurthala, India. He has published several research papers in leading international journals and conference proceedings, and presented papers at several prestigious academic conferences, such as IEEE and Springer. His research interests include power market, renewable energy sources, power system optimization, and condition monitoring of transformers.

SHAILENDRA MISHRA (Senior Member, IEEE) received the Master of Engineering degree (M.E.) in computer science and engineering from the Motilal Nehru National Institute of Technology (MNNIT)), India, in 2000, and the Ph.D. degree in computer science and engineering, in 2007. He is currently working as an Associate Professor with the Department of Computer Engineering, College of Computer and Information Science, Majmaah University, Majmaah, Saudi Arabia. He Published and presented more than 90 research papers in international journals and international conferences. His research interests include cloud and cyber security, SDN, and the IoT Security, and also conducting research on communication system and computer networks with performance evaluation and design of multiple access protocol for mobile communication networks. He is a Senior Member of ACM, Life Member of Institution of Engineers India (IEI), Indian Society of Technical Education (ISTE) and ACEEE.

SUNIL KUMAR SHARMA received the Ph.D. degree in mathematics from Gautam Buddh Technical University, Lucknow, India. He is currently an Associate Professor of mathematics with the College of Computer and Information Sciences, Majmaah University, Saudi Arabia. His research interests include cloud security, mathematical modelling, numerical computation of biomechanics of diarthrodial joints, multicriteria decision model for production systems, robot in the field of education, cloud security, and mathematical modelling of physical and biological problems in general and mathematical analysis. He is a member of AMC.